

Fractional QCQP With Applications in ML Steering Direction Estimation for Radar Detection

Antonio De Maio, *Senior Member, IEEE*, Yongwei Huang, *Member, IEEE*, Daniel P. Palomar, *Senior Member, IEEE*, Shuzhong Zhang, and Alfonso Farina, *Fellow, IEEE*

Abstract—This paper deals with the problem of estimating the steering direction of a signal, embedded in Gaussian disturbance, under a general quadratic inequality constraint, representing the uncertainty region of the steering. We resort to the maximum likelihood (ML) criterion and focus on two scenarios. The former assumes that the complex amplitude of the useful signal component fluctuates from snapshot to snapshot. The latter supposes that the useful signal keeps a constant amplitude within all the snapshots. We prove that the ML criterion leads in both cases to a fractional quadratically constrained quadratic problem (QCQP). In order to solve it, we first relax the problem into a constrained fractional semidefinite programming (SDP) problem which is shown equivalent, via the Charnes-Cooper transformation, to an SDP problem. Then, exploiting a suitable rank-one decomposition, we show that the SDP relaxation is tight and give a procedure to construct (in polynomial time) an optimal solution of the original problem from an optimal solution of the fractional SDP. We also assess the quality of the derived estimator through a comparison between its performance and the constrained Cramer Rao lower Bound (CRB). Finally, we give two applications of the proposed theoretical framework in the context of radar detection.

Index Terms—Constrained maximum likelihood steering direction estimation, fractional QCQP, radar applications.

I. INTRODUCTION

THE problem of estimating the steering direction vector is of relevant interest in some applications concerning radar detection and beamforming. In fact, there are several physical phenomena why the received steering vector is quite often not aligned with the nominal expected direction: such as pointing errors caused by the radar antenna which forms a beam not pointed in the exact desired direction; imperfect array calibration and

distorted antenna shape because of array imperfections; spatial multipath causing severe distortions in the presumed steering vector due to the presence of signals from several paths (coherent and incoherent local scattering); source wavefront distortion implied by the signal propagation through nonhomogeneous media; in-phase and quadrature components errors due to unbalanced lowpass filters; A/D sampling errors; dc bias; nonlinearities; and intermodulation products. In other words, there is some imperfect knowledge on the actual steering direction which is usually characterized in terms of an uncertainty region. Many adaptive radar signal processing methods that assume the exact knowledge of the signal array response vector often suffer a performance degradation, when the actual steering vector is not perfectly aligned with the nominal one (even small variations in the array manifold can reduce their performance).

In order to account for the quoted uncertainty, several estimation techniques have been proposed in open literature. For instance, with reference to beamforming applications, steering estimation is explicitly or implicitly addressed in [1]–[5]. As to the case of radar detection, steering vector estimation can be found in [6]–[12].

All the mentioned approaches focus on a specific uncertainty region and exploit some different objective functions to optimize. Actually, to the authors best knowledge, the problem of maximum likelihood (ML) joint estimation of signal amplitude and steering direction under a general steering uncertainty region, represented by a quadratic inequality constraint, has not yet been solved. To this end, in this paper, we consider steering direction ML estimation under a general quadratic inequality constraint (either convex or nonconvex) and the unit norm constraint which characterizes a direction vector. We focus on two distinct situations. One assumes that complex amplitude of the received useful signal changes from snapshot to snapshot, whereas the other accounts for a constant signal amplitude in all the received snapshots. Both the situations are of interest for radar signal processing applications concerning detection of range-spread targets [13], [14], multiple input multiple output (MIMO) target detection [15], [16], and radar detection using a general antenna array configuration with a mix of high- and low-gain beams [17]. We show that, upon concentration of the likelihood function over the amplitudes of the signal of interest, the steering direction estimation problem can be formulated as a fractional quadratically constrained quadratic problem (QCQP). Hence, in order to solve it, we first relax the problem into a constrained fractional semidefinite programming (SDP) which is proved equivalent to an SDP through the Charnes-Cooper transformation [18]. Then, we show that the relaxation is tight. Precisely, exploiting a suitable rank-one decomposition theorem [19], [20], we devise a technique aimed

Manuscript received March 13, 2010; accepted September 26, 2010. Date of publication October 14, 2010; date of current version December 17, 2010. The associate editor coordinating the review of this manuscript and approving it for publication was Prof. Dominic K. C. Ho. The work of D. P. Palomar and Y. Huang was supported by the Hong Kong RGC 618709 research grant. The work of S. Zhang was supported by National Natural Science Foundation of China (Grant 10771133).

A. De Maio is with the Dipartimento di Ingegneria Biomedica, Elettronica e delle Telecomunicazioni, Università degli Studi di Napoli “Federico II”, Napoli, Italy (e-mail: ademai@unina.it).

Y. Huang and D. P. Palomar are with the Department of Electronic and Computer Engineering, Hong Kong University of Science and Technology, Clear Water Bay, Kowloon, Hong Kong (e-mail: eeyw@ust.hk; palomar@ust.hk).

S. Zhang is with the Industrial and Systems Engineering Program, University of Minnesota, Minneapolis, MN 55455 USA, and also with the Department of Systems Engineering and Engineering Management, The Chinese University of Hong Kong, Shatin, Hong Kong (e-mail: zhang@se.cuhk.edu.hk).

A. Farina is with the SELEX Sistemi Integrati, Rome, Italy (e-mail: afa-rina@selex-si.com).

Color versions of one or more of the figures in this paper are available online at <http://ieeexplore.ieee.org>.

Digital Object Identifier 10.1109/TSP.2010.2087327

at recovering a solution of the original fractional QCQP from a solution of the fractional SDP relaxation. The overall procedure involves a polynomial computational complexity and, from the optimization theory point of view, this paper provides an efficient procedure to solve a general fractional QCQP with three homogeneous constraints, incorporating the specific rank-one decomposition technique [19].

We also provide considerations concerning the identifiability of the parameters in the considered estimation problem and evaluate the constrained Cramér–Rao lower bound (CRB) [21]. Finally, we apply the estimation framework to two radar detection problems. The former refers to radar detection of distributed targets; the latter to point-target detection with a radar using a general antenna array configuration with a mix of high- and low-gain beams. The analysis of the resulting decision rules in comparison with the classic one, assuming aligned nominal and actual steering directions, confirms the effectiveness of the approach.

The paper is organized as follows. In Section II, we formulate the steering direction estimation problem. In Section III, we discuss the identifiability of the model parameters and propose the new estimation procedure. Additionally, we derive the constrained CRB and assess, through an example, the quality of the estimates by the proposed algorithm. In Section IV, we apply the new estimation technique to two radar problems and analyze the performance of the receivers exploiting the robust estimator of the steering direction in place of the nominal one. Finally, conclusions and possible future research tracks are given in Section V.

Notation

We adopt the notation of using boldface for vectors \mathbf{a} (lower case), and matrices \mathbf{A} (upper case). The transpose and the conjugate transpose operators are denoted by the symbols $(\cdot)^T$ and $(\cdot)^\dagger$, respectively. $\text{tr}(\cdot)$, $\det(\cdot)$, $\text{rank}(\cdot)$, $\lambda_{\min}(\cdot)$, and $\lambda_{\max}(\cdot)$ are respectively the trace, the determinant, the rank, the minimum eigenvalue and the maximum eigenvalue of the square matrix argument. \mathbf{I} and $\mathbf{0}$ denote, respectively, the identity matrix and the matrix with zero entries (their size is determined from the context). \mathbb{R}^N , \mathbb{C}^N , and \mathbb{H}^N are respectively the sets of N -dimensional vectors of real numbers, N -dimensional vectors of complex numbers, and $N \times N$ Hermitian matrices. The curled inequality symbol \succeq (and its strict form \succ) is used to denote generalized matrix inequality: for any $\mathbf{A} \in \mathbb{H}^N$, $\mathbf{A} \succeq \mathbf{0}$ means that \mathbf{A} is a positive semidefinite matrix ($\mathbf{A} \succ \mathbf{0}$ for positive definiteness). The Euclidean norm of the vector \mathbf{x} is denoted by $\|\mathbf{x}\|$. The letter j represents the imaginary unit (i.e., $j = \sqrt{-1}$), while the letter i often serves as index in this paper. For any complex number x , we use $\Re(x)$ and $\Im(x)$ to denote, respectively, the real and the imaginary part of x , $|x|$ is the modulus of x , and x^* is the conjugate of x . Finally, \otimes denotes the Kronecker product and for any optimization problem \mathcal{P} , $v(\mathcal{P})$ represents its optimal value.

II. MAXIMUM LIKELIHOOD STEERING ESTIMATION: PROBLEM FORMULATION

We assume that data are collected from N sensors (for instance the receiving elements of an antenna array) and denote by \mathbf{z}_t , $t = 1, \dots, M$, the complex vectors of the received

samples which can be expressed as

$$\mathbf{z}_t = \alpha_t \mathbf{p} + \mathbf{w}_t, \quad t = 1, \dots, M, \quad (1)$$

where α_t 's are unknown complex parameters accounting for the channel propagation and signal strength, \mathbf{p} is the unit-norm steering vector of the signal of interest (i.e., $\mathbf{p} \in \mathcal{U}$, with $\mathcal{U} = \{\mathbf{p} \in \mathbb{C}^N : \|\mathbf{p}\|^2 = 1\}$), and \mathbf{w}_t 's are the disturbance components, modeled as statistically independent zero-mean complex circular Gaussian vectors with positive definite covariance matrix $E[\mathbf{w}_t \mathbf{w}_t^\dagger] = \mathbf{M}$. As to the α_t 's, we consider the following two different scenarios:

- 1) **Scenario 1.** It models $(\alpha_1, \dots, \alpha_M)$ as a vector of \mathbb{C}^M and is of relevant interest for radar detection of range-spread targets [13], [14], where the useful target might be spread in more than one range cell. In this case, α_t accounts for the backscattering coefficient of the scattering center in the t th range cell (if a high resolution radar is considered) or the radar cross section from the target in the t th range bin with reference to a formation of targets to be detected with a low-medium resolution radar.
- 2) **Scenario 2.** It assumes $\alpha_t = \alpha \beta_t$, $t = 1, \dots, M$, with β_t known complex numbers, while $\alpha \in \mathbb{C}$ is an unknown parameter. This signal model is useful in MIMO radar with colocated antennas [16, p. 11, eq. 1.29] and in modern radar systems [17] that have general antenna array configurations, containing a mix of high- and low-gain beams.

Additionally, we force \mathbf{p} to comply with a general (not necessarily convex) quadratic constraint, i.e.

$$\mathbf{p} \in \Omega = \mathcal{U} \cap \mathcal{C}, \quad \text{with } \mathcal{C} = \left\{ \mathbf{p} \in \mathbb{C}^N : \mathbf{p}^\dagger \mathbf{A} \mathbf{p} + 2\Re(\mathbf{b}^\dagger \mathbf{p}) + c \geq 0 \right\} \quad (2)$$

with $\mathbf{A} \in \mathbb{H}^N$, $\mathbf{b} \in \mathbb{C}^N$, and $c \in \mathbb{R}$.

The estimation of the steering direction is performed resorting to the maximum likelihood (ML) criterion. This technique is usually applied for radar detection applications in the presence of steering vector mismatches and/or when rejection capabilities (namely the possibility to reject signals which are outside an acceptance region centered around the expected steering direction) are required to the radar receiver¹. Otherwise stated, we are faced with the following optimization problem: [see (3) at the bottom of the next page], where $f(\mathbf{z}_1, \dots, \mathbf{z}_M | \alpha_1, \dots, \alpha_M, \mathbf{p}; \mathbf{M})$ and $f(\mathbf{z}_1, \dots, \mathbf{z}_M | \alpha, \mathbf{p}; \beta_1, \dots, \beta_M, \mathbf{M})$ are the joint probability density functions (pdf's) of the vectors $\mathbf{z}_1, \dots, \mathbf{z}_M$ under Scenario 1 and Scenario 2, respectively.

Exploiting the Gaussian assumption, the pdf for Scenario 1 can be written as

$$f(\mathbf{z}_1, \dots, \mathbf{z}_M | \alpha_1, \dots, \alpha_M, \mathbf{p}; \mathbf{M}) = \frac{1}{\pi^{NM} \det^M(\mathbf{M})} \times \exp \left[- \sum_{t=1}^M (\mathbf{z}_t - \alpha_t \mathbf{p})^\dagger \mathbf{M}^{-1} (\mathbf{z}_t - \alpha_t \mathbf{p}) \right] \quad (4)$$

¹The joint application of the ML criterion and the optimization theory to communications problems can be found in [22]–[24].

whereas that for Scenario 2, it is given by

$$f(\mathbf{z}_1, \dots, \mathbf{z}_M | \alpha, \mathbf{p}; \beta_1, \dots, \beta_M, \mathbf{M}) = \frac{1}{\pi^{NM} \det^M(\mathbf{M})} \times \exp \left[- \sum_{t=1}^M (\mathbf{z}_t - \alpha \beta_t \mathbf{p})^\dagger \mathbf{M}^{-1} (\mathbf{z}_t - \alpha \beta_t \mathbf{p}) \right]. \quad (5)$$

This implies that the ML estimation problem can be written as shown in (6) at the bottom of the page.

Before presenting the solution method to the above problems, it is necessary to highlight their practical importance and its relation to other existing methods. In radar detection, typical quadratic constraints that the vector \mathbf{p} has to comply with are

- **Conic Constraint:** $\mathcal{C} = \{ \mathbf{p} \in \mathbb{C}^N : |\mathbf{p}^\dagger \mathbf{p}_0|^2 \geq \gamma \|\mathbf{p}\|^2 \}$, where \mathbf{p}_0 is the nominal steering vector (assumed with unit norm) and $0 \leq \gamma \leq 1$. This is tantamount to limiting the minimum squared cosine angle between the actual and the nominal steering directions, namely \mathbf{p} has to lie in a conic region with axis \mathbf{p}_0 and whose aperture is ruled by γ . This kind of constraint is encountered in [6]–[8], [10], [12]. A pictorial representation of the constraint set Ω is given in Fig. 1(a).
- **Elliptical Constraint:** $\mathcal{C} = \{ \mathbf{p} \in \mathbb{C}^N : (\mathbf{p} - \mathbf{p}_0)^\dagger \mathbf{E} (\mathbf{p} - \mathbf{p}_0) \leq 1 \}$, where \mathbf{E} is a positive semidefinite matrix such that $\lambda_{\max}(\mathbf{E}) > 1/4$.² This is equivalent to assuming that \mathbf{p} lies into an ellipsoid whose center is the unit norm vector \mathbf{p}_0 and whose shape is ruled by the matrix \mathbf{E} . This constraint is commonly encountered in robust beamforming applications [2], [3], [5] and, for $\mathbf{E} = 1/\epsilon \mathbf{I}$, it reduces to the similarity constraint $\|\mathbf{p} - \mathbf{p}_0\|^2 \leq \epsilon$ [3], [4], [25], where $0 \leq \epsilon \leq 2$ rules the size of the similarity region. A pictorial representation of the resulting constraint set Ω is given in Fig. 1(b). Finally, in [26], some interesting procedures to determine the uncertainty ellipsoid are proposed and discussed.
- **Exterior Conic Constraint:** $\mathcal{C} = \{ \mathbf{p} \in \mathbb{C}^N : |\mathbf{p}^\dagger \mathbf{p}_0|^2 \leq \gamma \|\mathbf{p}\|^2 \}$, namely the useful signal lies outside a conic

²Otherwise $\Omega = \mathcal{U} \cap \mathcal{C}$ reduces to \mathcal{U} . Indeed, suppose that $\lambda_{\max}(\mathbf{E}) \leq 1/4$ and $\|\mathbf{p}\| = 1$. Then $1/4 \geq \lambda_{\max}(\mathbf{E}) \geq (\mathbf{p} - \mathbf{p}_0)^\dagger \mathbf{E} (\mathbf{p} - \mathbf{p}_0) / \|\mathbf{p} - \mathbf{p}_0\|^2 \geq (\mathbf{p} - \mathbf{p}_0)^\dagger \mathbf{E} (\mathbf{p} - \mathbf{p}_0) / (\|\mathbf{p}\| + \|\mathbf{p}_0\|)^2 = (\mathbf{p} - \mathbf{p}_0)^\dagger \mathbf{E} (\mathbf{p} - \mathbf{p}_0) / 4$, which implies $(\mathbf{p} - \mathbf{p}_0)^\dagger \mathbf{E} (\mathbf{p} - \mathbf{p}_0) \leq 1$; in other words, $\lambda_{\max}(\mathbf{E}) \leq 1/4$ and $\|\mathbf{p}\| = 1$ imply $\mathbf{p} \in \mathcal{C}$.

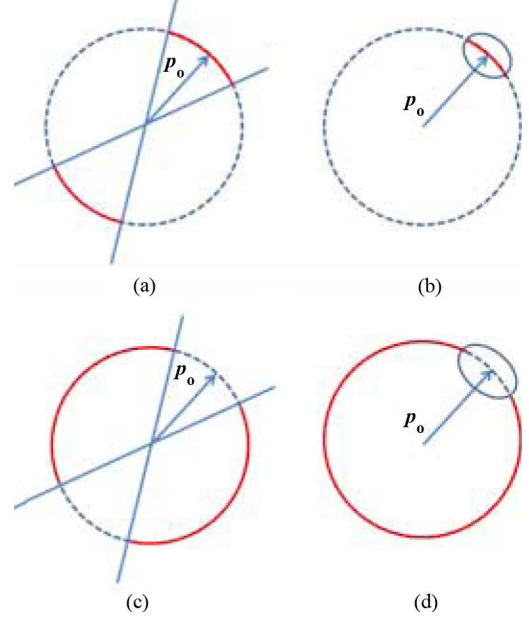


Fig. 1. Pictorial description of the set Ω for $N = 2$ and real observations.

region whose axis is the vector \mathbf{p}_0 . This constraint is of relevance in radar detection problems where rejection capabilities must be conferred to the receiver [9], [27], [28]. Specifically, it arises when it becomes necessary to discriminate between a useful signal lying in a conic region (H_1 hypothesis) and an interfering signal lying in the complement of the quoted region, namely the exterior of the cone (null hypothesis H_0). The graphic representation of the constraint Ω for this specific situation is given in Fig. 1(c).

- **Exterior Elliptical Constraint:** $\mathcal{C} = \{ \mathbf{p} \in \mathbb{C}^N : (\mathbf{p} - \mathbf{p}_0)^\dagger \mathbf{E} (\mathbf{p} - \mathbf{p}_0) \geq 1 \}$, $\lambda_{\max}(\mathbf{E}) \geq 1/4$,³ namely the useful signal has to lie outside of an ellipsoid whose center is the vector \mathbf{p}_0 [see Fig. 1(d) for the corresponding representation of Ω].

Evidently, the aforementioned four classes of quadratic constraints may or may not be convex, and the feasible regions are nonconvex, since they consist of one of the four classes of

³Otherwise, the set $\Omega = \mathcal{U} \cap \mathcal{C}$ is empty. Indeed, suppose that $\lambda_{\max}(\mathbf{E}) < 1/4$, $\mathbf{p} \in \mathcal{C}$ and $\|\mathbf{p}\| = 1$, and then one gets the contradiction: $1/4 > \lambda_{\max}(\mathbf{E}) \geq (\mathbf{p} - \mathbf{p}_0)^\dagger \mathbf{E} (\mathbf{p} - \mathbf{p}_0) / \|\mathbf{p} - \mathbf{p}_0\|^2 \geq (\mathbf{p} - \mathbf{p}_0)^\dagger \mathbf{E} (\mathbf{p} - \mathbf{p}_0) / (\|\mathbf{p}\| + \|\mathbf{p}_0\|)^2 \geq 1/4$.

$$\begin{aligned} & \underset{(\alpha_1, \dots, \alpha_M) \in \mathbb{C}^M}{\text{maximize}} \underset{\mathbf{p} \in \Omega}{\text{maximize}} f(\mathbf{z}_1, \dots, \mathbf{z}_M | \alpha_1, \dots, \alpha_M, \mathbf{p}; \mathbf{M}), \text{ Scenario 1} \\ & \underset{\alpha \in \mathbb{C}}{\text{maximize}} \underset{\mathbf{p} \in \Omega}{\text{maximize}} f(\mathbf{z}_1, \dots, \mathbf{z}_M | \alpha, \mathbf{p}; \beta_1, \dots, \beta_M, \mathbf{M}), \text{ Scenario 2} \end{aligned} \quad (3)$$

$$\mathcal{P}_{\text{ML}} \begin{cases} \underset{(\alpha_1, \dots, \alpha_M) \in \mathbb{C}^M}{\text{minimize}} \underset{\mathbf{p} \in \Omega}{\text{minimize}} \sum_{t=1}^M (\mathbf{z}_t - \alpha_t \mathbf{p})^\dagger \mathbf{M}^{-1} (\mathbf{z}_t - \alpha_t \mathbf{p}), & \text{Scenario 1} \\ \underset{\alpha \in \mathbb{C}}{\text{minimize}} \underset{\mathbf{p} \in \Omega}{\text{minimize}} \sum_{t=1}^M (\mathbf{z}_t - \alpha \beta_t \mathbf{p})^\dagger \mathbf{M}^{-1} (\mathbf{z}_t - \alpha \beta_t \mathbf{p}), & \text{Scenario 2.} \end{cases} \quad (6)$$

quadratic constraints and the norm constraint $\|\mathbf{p}\| = 1$. Furthermore, the objective function of problem \mathcal{P}_{ML} is neither convex nor quadratic. In fact, consider the simplest case: $M = 1$, and the objective function (for Scenario 1) becomes

$$(z_1 - \alpha_1 \mathbf{p})^\dagger \mathbf{M}^{-1} (z_1 - \alpha_1 \mathbf{p})$$

(set $\beta_t = 1$ for Scenario 2). Evaluating the Hessian matrix

$$\begin{bmatrix} |\alpha_1|^2 \mathbf{M}^{-1} & \alpha_1 \mathbf{M}^{-1} \mathbf{p} - \mathbf{M}^{-1} z_1 \\ \alpha_1^\dagger \mathbf{p}^\dagger \mathbf{M}^{-1} - z_1^\dagger \mathbf{M}^{-1} & \mathbf{p}^\dagger \mathbf{M}^{-1} \mathbf{p} \end{bmatrix} \quad (7)$$

it is neither a constant matrix nor a positive semidefinite matrix for some $(\mathbf{p}, \alpha) \in \Omega \times \mathbb{C}$.⁴ In other words, the objective function is neither quadratic nor convex; thus problem \mathcal{P}_{ML} is a nonconvex program (neither a QCQP), and seems difficult to solve. However, we will show that the problem can be solved efficiently. Precisely, in the next section, we will show that problem \mathcal{P}_{ML} , after concentration over the complex amplitudes α_t 's for Scenario 1 (over α for Scenario 2) is equivalent to a fractional SDP, whose solutions can be obtained by solving its equivalent SDP via the so-called Charnes-Cooper transformation [18]. Then, we retrieve an optimal solution of \mathcal{P}_{ML} from an optimal solution to the equivalent fractional SDP through specific rank-one decompositions [19].

III. IDENTIFIABILITY, SOLUTION TO THE ML STEERING DIRECTION ESTIMATION PROBLEM, AND CONSTRAINED CRB

In this section, we first address the identifiability of the model parameters, then we introduce the new algorithm which in polynomial time provides a solution to the estimation problem, and, finally, we assess the quality of the derived estimate through a comparison with the constrained CRB for the considered problem.

A. Identifiability of the Model Parameters

Identifiability refers to the study of the solution to the estimation problem in the noiseless case. It is basically a consistency aspect which allows to understand whether the solution is unique in the ideal case of no noise. With reference to our problem, the identifiability equations can be written as

$$\alpha_t \mathbf{p} = \check{\alpha}_t \check{\mathbf{p}}, \quad t = 1, \dots, M, \quad \text{Scenario 1} \quad (8)$$

⁴For example, at the points $(0, \mathbf{p})$, $(\alpha_1, 0)$, $(0, 0)$, the Hessian matrix (7) is not positive semidefinite.

($\alpha \mathbf{p} = \check{\alpha} \check{\mathbf{p}}$ for Scenario 2). Assuming that $\check{\mathbf{p}} \in \Omega$ and $\check{\alpha}_t$'s ($\check{\alpha}$ for Scenario 2) are complex numbers, the identifiability of the parameters α_t , $t = 1, \dots, M$, and \mathbf{p} holds if (8) has a unique solution with $\mathbf{p} \in \Omega$. Evidently this is not the case since both $\check{\alpha}_t$'s ($\check{\alpha}$ for Scenario 2) $\check{\mathbf{p}}$ and $\check{\alpha}_t e^{j\phi_g}$'s ($\check{\alpha} e^{j\phi_g}$ for Scenario 2) $\check{\mathbf{p}} e^{-j\phi_g}$ with

$$\phi_g = \begin{cases} \arg(\mathbf{b}^\dagger \check{\mathbf{p}}) & \text{if } \mathbf{b} \neq \mathbf{0} \\ \arg(\mathbf{e}_1^\dagger \check{\mathbf{p}}) & \text{if } \mathbf{b} = \mathbf{0} \end{cases}$$

[where \mathbf{b} is defined in (2)] and $\mathbf{e}_1 = [1, 0, \dots, 0]^T$, are solutions of (8). Nevertheless, we can easily obtain identifiability imposing a further constraint on \mathbf{p} , i.e.

$$\begin{aligned} \Im(\mathbf{b}^\dagger \mathbf{p}) &= 0, & \Re(\mathbf{b}^\dagger \mathbf{p}) &\geq 0 & \text{if } \mathbf{b} \neq \mathbf{0}, \\ \Im(\mathbf{e}_1^\dagger \mathbf{p}) &= 0, & \Re(\mathbf{e}_1^\dagger \mathbf{p}) &\geq 0 & \text{if } \mathbf{b} = \mathbf{0}. \end{aligned} \quad (9)$$

With this additional constraint the phase ambiguity is eliminated and the solution of (8) is unique thanks to the unit norm condition.

It is worth pointing out that if the last constraint (9) is added to the estimation problem of Section II, the algorithm, we will propose in the next subsection, can be still applied to obtain the ML estimates of the parameters provided that its output $(\alpha_{1\text{ML}}, \dots, \alpha_{M\text{ML}}, \mathbf{p}_{\text{ML}})$ ($(\alpha_{\text{ML}}, \mathbf{p}_{\text{ML}})$ for Scenario 2) is phase rotated in order to comply with (9). In the following, the set Ω augmented with (9) is denoted by Ω_a .

B. Solution to the ML Steering Direction Estimation Problem

In this subsection, we show how the solution to the ML steering estimation problem can be obtained in polynomial time. To this end, we observe that problem \mathcal{P}_{ML} can be equivalently rewritten as shown in (10) at the bottom of the page. The inner minimization is direct, i.e., for Scenario 1

$$\begin{aligned} & -\frac{\mathbf{p}^\dagger \mathbf{M}^{-1} z_t z_t^\dagger \mathbf{M}^{-1} \mathbf{p}}{\mathbf{p}^\dagger \mathbf{M}^{-1} \mathbf{p}} + z_t^\dagger \mathbf{M}^{-1} z_t \\ & = \underset{\alpha_t \in \mathbb{C}}{\text{minimize}} (z_t - \alpha_t \mathbf{p})^\dagger \mathbf{M}^{-1} (z_t - \alpha_t \mathbf{p}) \end{aligned} \quad (11)$$

and the minimal value is attained at

$$\alpha_t^* = \frac{\mathbf{p}^\dagger \mathbf{M}^{-1} z_t}{\mathbf{p}^\dagger \mathbf{M}^{-1} \mathbf{p}}. \quad (12)$$

$$\mathcal{P} \begin{cases} \underset{\mathbf{p} \in \Omega}{\text{minimize}} \sum_{t=1}^M \underset{\alpha_t \in \mathbb{C}}{\text{minimize}} (z_t - \alpha_t \mathbf{p})^\dagger \mathbf{M}^{-1} (z_t - \alpha_t \mathbf{p}), & \text{Scenario 1} \\ \underset{\mathbf{p} \in \Omega}{\text{minimize}} \sum_{t=1}^M \underset{\alpha \in \mathbb{C}}{\text{minimize}} (z_t - \alpha \beta_t \mathbf{p})^\dagger \mathbf{M}^{-1} (z_t - \alpha \beta_t \mathbf{p}), & \text{Scenario 2.} \end{cases} \quad (10)$$

For Scenario 2

$$-\frac{\mathbf{p}^\dagger \mathbf{M}^{-1} \mathbf{q} \mathbf{q}^\dagger \mathbf{M}^{-1} \mathbf{p}}{\mathbf{p}^\dagger \mathbf{M}^{-1} \mathbf{p}} + \sum_{t=1}^M z_t^\dagger \mathbf{M}^{-1} z_t$$

$$= \underset{\alpha \in \mathbb{C}}{\text{minimize}} \sum_{t=1}^M (z_t - \alpha \beta_t \mathbf{p})^\dagger \mathbf{M}^{-1} (z_t - \alpha \beta_t \mathbf{p}) \quad (13)$$

with

$$\mathbf{q} = \frac{\sum_{t=1}^M \beta_t^\dagger z_t}{\sqrt{\sum_{t=1}^M |\beta_t|^2}},$$

and the minimal value is attained at

$$\alpha_t^* = \frac{\sum_{t=1}^M \beta_t^\dagger \mathbf{p}^\dagger \mathbf{M}^{-1} z_t}{\sum_{t=1}^M |\beta_t|^2 \mathbf{p}^\dagger \mathbf{M}^{-1} \mathbf{p}} = \frac{\mathbf{p}^\dagger \mathbf{M}^{-1} \mathbf{q}}{\mathbf{p}^\dagger \mathbf{M}^{-1} \mathbf{p} \sqrt{\sum_{t=1}^M |\beta_t|^2}}. \quad (14)$$

Therefore, \mathcal{P} amounts to

$$\sum_{t=1}^M z_t^\dagger \mathbf{M}^{-1} z_t + \underset{\mathbf{p} \in \Omega}{\text{minimize}} -\frac{\mathbf{p}^\dagger \mathbf{M}^{-1} \mathbf{S} \mathbf{M}^{-1} \mathbf{p}}{\mathbf{p}^\dagger \mathbf{M}^{-1} \mathbf{p}}$$

$$= \sum_{t=1}^M z_t^\dagger \mathbf{M}^{-1} z_t - \underset{\mathbf{p} \in \Omega}{\text{maximize}} \frac{\mathbf{p}^\dagger \mathbf{M}^{-1} \mathbf{S} \mathbf{M}^{-1} \mathbf{p}}{\mathbf{p}^\dagger \mathbf{M}^{-1} \mathbf{p}} \quad (15)$$

where

$$\mathbf{S} = \begin{cases} \sum_{t=1}^M z_t z_t^\dagger, & \text{Scenario 1} \\ \mathbf{q} \mathbf{q}^\dagger, & \text{Scenario 2.} \end{cases} \quad (16)$$

Now, let us focus on solving the fractional QCQP

$$\mathcal{P}_1 \left\{ \underset{\mathbf{p} \in \Omega}{\text{maximize}} \frac{\mathbf{p}^\dagger \mathbf{M}^{-1} \mathbf{S} \mathbf{M}^{-1} \mathbf{p}}{\mathbf{p}^\dagger \mathbf{M}^{-1} \mathbf{p}} \right. \quad (17)$$

where Ω is defined by (2). The homogenized version of \mathcal{P}_1 is shown in

$$\mathcal{P}_2 \left\{ \begin{array}{l} \underset{\mathbf{p}, t}{\text{maximize}} \quad \frac{\text{tr} \left(\begin{bmatrix} \mathbf{M}^{-1} \mathbf{S}^\dagger \mathbf{M}^{-1} & \mathbf{0} \\ \mathbf{0} & 0 \end{bmatrix} \begin{bmatrix} \mathbf{p} \mathbf{p}^\dagger & \mathbf{p} t^* \\ \mathbf{p}^\dagger t & |t|^2 \end{bmatrix} \right)}{\text{tr} \left(\begin{bmatrix} \mathbf{M}^{-1} & \mathbf{0} \\ \mathbf{0} & 0 \end{bmatrix} \begin{bmatrix} \mathbf{p} \mathbf{p}^\dagger & \mathbf{p} t^* \\ \mathbf{p}^\dagger t & |t|^2 \end{bmatrix} \right)} \\ \text{subject to} \quad \text{tr} \left(\begin{bmatrix} \mathbf{A} & \mathbf{b} \\ \mathbf{b}^\dagger & c \end{bmatrix} \begin{bmatrix} \mathbf{p} \mathbf{p}^\dagger & \mathbf{p} t^* \\ \mathbf{p}^\dagger t & |t|^2 \end{bmatrix} \right) \geq 0 \\ \text{tr} \left(\begin{bmatrix} \mathbf{I} & \mathbf{0} \\ \mathbf{0} & 0 \end{bmatrix} \begin{bmatrix} \mathbf{p} \mathbf{p}^\dagger & \mathbf{p} t^* \\ \mathbf{p}^\dagger t & |t|^2 \end{bmatrix} \right) = 1 \\ \text{tr} \left(\begin{bmatrix} \mathbf{0} & \mathbf{0} \\ \mathbf{0} & 1 \end{bmatrix} \begin{bmatrix} \mathbf{p} \mathbf{p}^\dagger & \mathbf{p} t^* \\ \mathbf{p}^\dagger t & |t|^2 \end{bmatrix} \right) = 1 \\ \mathbf{p} \in \mathbb{C}^N, t \in \mathbb{C}. \end{array} \right. \quad (18)$$

We highlight that the two problems \mathcal{P}_1 and \mathcal{P}_2 have the same optimal value (i.e., $v(\mathcal{P}_1) = v(\mathcal{P}_2)$), and \mathbf{p}^*/t^* is optimal to \mathcal{P}_1 if (\mathbf{p}^*, t^*) solves \mathcal{P}_2 . In fact, it is evident that $v(\mathcal{P}_1) \leq v(\mathcal{P}_2)$; on the other hand, the objective function of \mathcal{P}_1 evaluated at \mathbf{p}^*/t^* is equal to the optimal value of \mathcal{P}_2 , provided that (\mathbf{p}^*, t^*) is an optimal solution for \mathcal{P}_2 .

The SDP relaxation of \mathcal{P}_2 is

$$\mathcal{P}_3 \left\{ \begin{array}{l} \underset{\mathbf{W}}{\text{maximize}} \quad \frac{\text{tr}(\mathbf{Q}_{-1} \mathbf{W})}{\text{tr}(\mathbf{Q}_0 \mathbf{W})} \\ \text{subject to} \quad \text{tr}(\mathbf{Q}_1 \mathbf{W}) \geq 0 \\ \text{tr}(\mathbf{Q}_2 \mathbf{W}) = 1 \\ \text{tr}(\mathbf{Q}_3 \mathbf{W}) = 1 \\ \mathbf{W} \succeq \mathbf{0} \end{array} \right. \quad (19)$$

where \mathbf{Q}_i 's, are defined as follows:

$$\mathbf{Q}_{-1} = \begin{bmatrix} \mathbf{M}^{-1} \mathbf{S} \mathbf{M}^{-1} & \mathbf{0} \\ \mathbf{0} & 0 \end{bmatrix}, \quad \mathbf{Q}_0 = \begin{bmatrix} \mathbf{M}^{-1} & \mathbf{0} \\ \mathbf{0} & 0 \end{bmatrix} \quad (20)$$

and

$$\mathbf{Q}_1 = \begin{bmatrix} \mathbf{A} & \mathbf{b} \\ \mathbf{b}^\dagger & c \end{bmatrix}, \quad \mathbf{Q}_2 = \begin{bmatrix} \mathbf{I} & \mathbf{0} \\ \mathbf{0} & 0 \end{bmatrix}, \quad \mathbf{Q}_3 = \begin{bmatrix} \mathbf{0} & \mathbf{0} \\ \mathbf{0} & 1 \end{bmatrix}. \quad (21)$$

It is known that the single-ratio fractional SDP \mathcal{P}_3 can be iteratively solved by either the Dinkelbach algorithm (for instance see [29] and [30]) or the bisection search (see [31]). In this paper, we will solve \mathcal{P}_3 in one single shot by resorting to a variation of the so-called Charnes-Cooper variable transformation which was originally introduced in [18]. By the Charnes-Cooper variable transformation, one can replace a linear fractional program with at most two straightforward linear programs that differ from each other by only a change of sign in the objective function and in one constraint, and thus achieves a global optimal solution of the linear fractional program by solving at most two linear programs. By using the idea of Charnes and Cooper's transformation, and considering that the denominator of the fractional SDP \mathcal{P}_3 is always positive, we can convert the fractional SDP into an equivalent SDP. Precisely, let us define the transformed variable $\mathbf{X} = s\mathbf{W}$, where $s \geq 0$ complies with $\text{tr}(\mathbf{Q}_0(s\mathbf{W})) = 1$. Hence, multiplying by s the numerator and the denominator of the objective function in \mathcal{P}_3 , we obtain the SDP problem

$$\mathcal{P}_4 \left\{ \begin{array}{l} \underset{\mathbf{X}, s}{\text{maximize}} \quad \text{tr}(\mathbf{Q}_{-1} \mathbf{X}) \\ \text{subject to} \quad \text{tr}(\mathbf{Q}_0 \mathbf{X}) = 1 \\ \text{tr}(\mathbf{Q}_1 \mathbf{X}) \geq 0 \\ \text{tr}(\mathbf{Q}_2 \mathbf{X}) = s \\ \text{tr}(\mathbf{Q}_3 \mathbf{X}) = s \\ \mathbf{X} \succeq \mathbf{0}, s \geq 0. \end{array} \right. \quad (22)$$

In the following, we show that the fractional SDP \mathcal{P}_3 is equivalent to the SDP (22), in the sense that they have the equal optimal value and optimal solutions differ from one to another by a constant. In order to claim the equivalence between \mathcal{P}_3 and \mathcal{P}_4 , we first prove three lemmas showing that the two problems are

solvable⁵ (Lemmas 3.1 and 3.2), and that they share the same optimal value (Lemma 3.3) even if the optimal solutions differ up to a scalar whose expression is specified in Lemma 3.3.

Lemma 3.1: The fractional SDP problem \mathcal{P}_3 is solvable.

Proof: See Appendix A. ■

Lemma 3.2: The SDP problem \mathcal{P}_4 is solvable.

Proof: See Appendix B. ■

Lemma 3.3: Problems \mathcal{P}_3 and \mathcal{P}_4 have the equal optimal value. Furthermore, if \mathbf{X}^* solves \mathcal{P}_3 , then $(\mathbf{X}^*/\text{tr}(\mathbf{Q}_0\mathbf{X}^*), 1/\text{tr}(\mathbf{Q}_0\mathbf{X}^*))$ solves \mathcal{P}_4 ; if (\mathbf{X}^*, s^*) solves \mathcal{P}_4 , then \mathbf{X}^*/s^* solves \mathcal{P}_3 .

Proof: See Appendix C. ■

Once an optimal solution \mathbf{X}^* of \mathcal{P}_3 is obtained, we can check the rank of \mathbf{X}^* . If \mathbf{X}^* is of rank one, then the solution is a global optimal solution of the fractional QCQP \mathcal{P}_2 since \mathcal{P}_3 is a relaxation of \mathcal{P}_2 by dropping the rank-one constraint. If \mathbf{X}^* is of rank higher than one, we will construct a rank-one optimal solution $\mathbf{x}^*(\mathbf{x}^*)^\dagger$ of \mathcal{P}_3 by a recent matrix decomposition theorem [19]⁶. Then, the solution \mathbf{x}^* is an optimal solution of \mathcal{P}_2 . In other words, the SDP relaxation (19) is tight. Specifically, in order to construct a rank-one optimal solution to \mathcal{P}_3 , we use the rank-one matrix decomposition theorem [19, Theorem 2.3], which is cited as the following lemma.

Lemma 3.4: Let \mathbf{X} be a nonzero $N \times N$ ($N \geq 3$) complex Hermitian positive semidefinite matrix and \mathbf{A}_i be Hermitian matrix, $i = 1, 2, 3, 4$, and suppose that $(\text{tr}(\mathbf{Y}\mathbf{A}_1), \text{tr}(\mathbf{Y}\mathbf{A}_2), \text{tr}(\mathbf{Y}\mathbf{A}_3), \text{tr}(\mathbf{Y}\mathbf{A}_4)) \neq (0, 0, 0, 0)$ for any nonzero complex Hermitian positive semidefinite matrix \mathbf{Y} of size $N \times N$. Then,

- if $\text{rank}(\mathbf{X}) \geq 3$, one can find, in polynomial time, a rank-one matrix $\mathbf{x}\mathbf{x}^\dagger$ such that \mathbf{x} (synthetically denoted as $\mathbf{x} = \mathcal{D}_1(\mathbf{X}, \mathbf{A}_1, \mathbf{A}_2, \mathbf{A}_3, \mathbf{A}_4)$) is in $\text{range}(\mathbf{X})$, and

$$\mathbf{x}^\dagger \mathbf{A}_i \mathbf{x} = \text{tr}(\mathbf{X}\mathbf{A}_i), \quad i = 1, 2, 3, 4;$$

- if $\text{rank}(\mathbf{X}) = 2$, for any \mathbf{z} not in the range space of \mathbf{X} , one can find a rank-one matrix $\mathbf{x}\mathbf{x}^\dagger$ such that \mathbf{x} (synthetically denoted as $\mathbf{x} = \mathcal{D}_2(\mathbf{X}, \mathbf{A}_1, \mathbf{A}_2, \mathbf{A}_3, \mathbf{A}_4)$) is in the linear subspace spanned by $\{\mathbf{z}\} \cup \text{range}(\mathbf{X})$, and

$$\mathbf{x}^\dagger \mathbf{A}_i \mathbf{x} = \text{tr}(\mathbf{X}\mathbf{A}_i), \quad i = 1, 2, 3, 4.$$

Let us check the applicability of the lemma to both \mathbf{X}^* and the matrix parameters of \mathcal{P}_3 . Indeed, the condition $N \geq 3$ is mild and practical. Now, in order to verify

$$\begin{aligned} &(\text{tr}(\mathbf{Y}\mathbf{Q}_1), \text{tr}(\mathbf{Y}\mathbf{Q}_2), \text{tr}(\mathbf{Y}\mathbf{Q}_3), \text{tr}(\mathbf{Y}\mathbf{Q}_4)) \\ &\neq (0, 0, 0, 0), \text{ for any nonzero } \mathbf{Y} \succeq 0 \end{aligned}$$

it suffices to prove that there is $(a_1, a_2, a_3, a_4) \in \mathbb{R}^4$ such that

$$a_1\mathbf{Q}_1 + a_2\mathbf{Q}_2 + a_3\mathbf{Q}_3 + a_4\mathbf{Q}_4 \succ 0,$$

⁵By ‘‘solvable,’’ we mean that the problem is feasible and bounded, and the optimal value is attained; see [32, page 13].

⁶Note that once getting an optimal rank-one solution of (19) (as stated in **Algorithm 1** herein), we can give an optimal rank-one solution of (22) too, according to Lemma 3.3.

where

$$\mathbf{Q}_4 = \begin{bmatrix} \mathbf{M}^{-1}\mathbf{S}\mathbf{M}^{-1} - v(\mathcal{P}_3)\mathbf{M}^{-1} & \mathbf{0} \\ \mathbf{0} & 0 \end{bmatrix}.$$

But this is evident for the matrix parameters⁷ of \mathcal{P}_2 .

Algorithm 1 summarizes the procedure leading to an optimal solution \mathbf{p}^* of \mathcal{P}_1 .

Algorithm 1: Algorithm for Fractional QCQP \mathcal{P}_1

Input: $\mathbf{M}^{-1}, \mathbf{S}, \mathbf{Q}_1$.

Output: An optimal solution \mathbf{p}^* of \mathcal{P}_1 .

- 1: solve SDP \mathcal{P}_4 finding an optimal solution (\mathbf{X}^*, s^*) and the optimal value v^* ;
 - 2: let $\mathbf{X}^* := \mathbf{X}^*/s^*$;
 - 3: **if** $\text{rank}(\mathbf{X}^*) = 1$ **then**
 - 4: perform an eigen-decomposition $\mathbf{X}^* = \mathbf{x}^*(\mathbf{x}^*)^\dagger$,
 where $\mathbf{x}^* = \begin{bmatrix} \mathbf{p}^* \\ t^* \end{bmatrix}$; output $\mathbf{p}^* := \mathbf{p}^*/t^*$ and terminate.
 - 5: **else if** $\text{rank}(\mathbf{X}^*) = 2$ **then**
 - 6: find
 $\mathbf{x}^* = \mathcal{D}_2\left(\mathbf{X}^*, \begin{bmatrix} \mathbf{M}^{-1}\mathbf{S}\mathbf{M}^{-1} - v^*\mathbf{M}^{-1} & \mathbf{0} \\ \mathbf{0} & 0 \end{bmatrix}, \begin{bmatrix} \mathbf{A} & \mathbf{b} \\ \mathbf{b}^\dagger & c \end{bmatrix}, \begin{bmatrix} \mathbf{I} & \mathbf{0} \\ \mathbf{0} & 0 \end{bmatrix}, \begin{bmatrix} \mathbf{0} & \mathbf{0} \\ \mathbf{0} & 1 \end{bmatrix}\right)$;
 - 7: **else**
 - 8: find
 $\mathbf{x}^* = \mathcal{D}_1\left(\mathbf{X}^*, \begin{bmatrix} \mathbf{M}^{-1}\mathbf{S}\mathbf{M}^{-1} - v^*\mathbf{M}^{-1} & \mathbf{0} \\ \mathbf{0} & 0 \end{bmatrix}, \begin{bmatrix} \mathbf{A} & \mathbf{b} \\ \mathbf{b}^\dagger & c \end{bmatrix}, \begin{bmatrix} \mathbf{I} & \mathbf{0} \\ \mathbf{0} & 0 \end{bmatrix}, \begin{bmatrix} \mathbf{0} & \mathbf{0} \\ \mathbf{0} & 1 \end{bmatrix}\right)$;
 - 9: **end**
 - 10: let $\mathbf{x}^* = \begin{bmatrix} \mathbf{p}^* \\ t^* \end{bmatrix}$; output $\mathbf{p}^* := \mathbf{p}^*/t^*$.
-

The computational complexity, connected with the implementation of Algorithm 1⁸ includes the complexity of solving SDP \mathcal{P}_4 , which is of order $O(N^{3.5} \log(1/\eta))$ (see [32, p. 250]), where η is a prefixed accuracy, and the complexity of the specific rank-one decomposition procedure which is $O(N^3)$.

Given an optimal solution \mathbf{p}^* of \mathcal{P}_1 , it follows by (12) that for Scenario 1,

$$(\alpha_1^*, \dots, \alpha_M^*, \mathbf{p}^*) = \left(\frac{(\mathbf{p}^*)^\dagger \mathbf{M}^{-1} \mathbf{z}_1}{(\mathbf{p}^*)^\dagger \mathbf{M}^{-1} \mathbf{p}^*}, \dots, \frac{(\mathbf{p}^*)^\dagger \mathbf{M}^{-1} \mathbf{z}_M}{(\mathbf{p}^*)^\dagger \mathbf{M}^{-1} \mathbf{p}^*}, \mathbf{p}^* \right)$$

and for Scenario 2,

$$(\alpha^*, \mathbf{p}^*) = \left(\frac{(\mathbf{p}^*)^\dagger \mathbf{M}^{-1} \mathbf{q}}{\sqrt{\sum_{t=1}^M |\beta_t|^2 (\mathbf{p}^*)^\dagger \mathbf{M}^{-1} \mathbf{p}^*}}, \mathbf{p}^* \right),$$

⁷In fact, taking $a_1 = a_4 = 0$ and $a_3 = a_2 = 1$, then $a_1\mathbf{Q}_1 + a_2\mathbf{Q}_2 + a_3\mathbf{Q}_3 + a_4\mathbf{Q}_4 = \mathbf{I} \succ 0$.

⁸We highlight that Algorithm 1 includes solving the SDP relaxation problem \mathcal{P}_4 , performing a similar Charnes-Cooper transformation, and some matrix rank-one decompositions which are specified in Lemma 3.4. In [19, Algorithm 1] demonstrates how to decompose a positive semidefinite matrix according to [19, Th. 2.1]. In fact, [19, Th. 2.1] and [20, Th. 2.1] are the core of the rank-one decompositions described in [19, Th. 2.3] (cited by Lemma 3.4 herein).

is an optimal solution of problem \mathcal{P}_{ML} . Algorithm 2 describes the procedure to find the ML estimates (i.e., the optimal solution to \mathcal{P}_{ML}).

Algorithm 2: Finding an Optimal Solution of \mathcal{P}_{ML}

Input: $\mathbf{M}^{-1}, \mathbf{z}_1, \dots, \mathbf{z}_M, \mathbf{Q}_1$.

Output: An optimal solution $(\alpha_{1_{\text{ML}}}, \dots, \alpha_{M_{\text{ML}}}, \mathbf{p}_{\text{ML}})$ for Scenario 1 ($(\alpha_{\text{ML}}, \mathbf{p}_{\text{ML}})$ for Scenario 2).

- 1: define \mathbf{S} as (16);
 - 2: $\mathbf{p}^* = \text{Algorithm 1}(\mathbf{M}, \mathbf{S}, \mathbf{Q}_1)$.
 - 3: let $\alpha_{t_{\text{ML}}} := (\mathbf{p}^*)^\dagger \mathbf{M}^{-1} \mathbf{z}_t / (\mathbf{p}^*)^\dagger \mathbf{M}^{-1} \mathbf{p}^*$, $t = 1, \dots, M$, and $\mathbf{p}_{\text{ML}} := \mathbf{p}^*$ for Scenario 1 ($\alpha_{\text{ML}} := (\mathbf{p}^*)^\dagger \mathbf{M}^{-1} \mathbf{q} / \sqrt{\sum_{t=1}^M |\beta_t|^2} (\mathbf{p}^*)^\dagger \mathbf{M}^{-1} \mathbf{p}^*$, and $\mathbf{p}_{\text{ML}} := \mathbf{p}^*$ for Scenario 2).
-

C. Constrained CRB and Accuracy of the Proposed Estimator

In this subsection, we evaluate the constrained CRB for the estimation of \mathbf{p} and analyze the quality of the estimator proposed in the previous subsection through a comparison between its accuracy and the CRB. Assuming that \mathbf{p} is a regular point of the inequality constraints involved in Ω_a , the CRB under the constraint $\mathbf{p} \in \Omega_a$ is identical to that under the constraints $\mathbf{p} \in \mathcal{U}$ and $\Im(\mathbf{b}_a^\dagger \mathbf{p}) = 0$ (with $\mathbf{b}_a = \mathbf{b}$ if $\mathbf{b} \neq \mathbf{0}$ and $\mathbf{b}_a = \mathbf{e}_1$ otherwise) [33]. In other words, only the equality constraints have to be considered. In the following, we derive the CRB exploiting the technique proposed in [21].

Let us define $\boldsymbol{\theta}_p = [\Re(\mathbf{p})^T, \Im(\mathbf{p})^T]^T$, $\boldsymbol{\theta}_\alpha = [\Re(\alpha_1), \Im(\alpha_1), \dots, \Re(\alpha_M), \Im(\alpha_M)]^T$ for Scenario 1 ($\boldsymbol{\theta}_\alpha = [\Re(\alpha), \Im(\alpha)]^T$ for Scenario 2), and $\boldsymbol{\theta} = [\boldsymbol{\theta}_p^T, \boldsymbol{\theta}_\alpha^T]^T$. After some standard algebra, the Fisher Information Matrix (FIM) [34] \mathbf{J} can be written as

$$\mathbf{J}(\boldsymbol{\theta}) = \begin{bmatrix} \mathbf{J}_{\boldsymbol{\theta}_p, \boldsymbol{\theta}_p}(\boldsymbol{\theta}) & \mathbf{J}_{\boldsymbol{\theta}_p, \boldsymbol{\theta}_\alpha}(\boldsymbol{\theta}) \\ \mathbf{J}_{\boldsymbol{\theta}_\alpha, \boldsymbol{\theta}_p}(\boldsymbol{\theta}) & \mathbf{J}_{\boldsymbol{\theta}_\alpha, \boldsymbol{\theta}_\alpha}(\boldsymbol{\theta}) \end{bmatrix}$$

where

$$\mathbf{J}_{\boldsymbol{\theta}_p, \boldsymbol{\theta}_p}(\boldsymbol{\theta}) = 2\xi \Re \left(\begin{bmatrix} 1 & j \\ -j & 1 \end{bmatrix} \otimes \mathbf{M}^{-1} \right)$$

with $\xi = \sum_{t=1}^M |\alpha_t|^2$ for Scenario 1 and $\xi = |\alpha|^2 \sum_{t=1}^M |\beta_t|^2$ for Scenario 2;

$$\mathbf{J}_{\boldsymbol{\theta}_\alpha, \boldsymbol{\theta}_\alpha}(\boldsymbol{\theta}) = \begin{cases} 2\mathbf{p}^\dagger \mathbf{M}^{-1} \mathbf{p} \mathbf{I}_{2M} \\ 2 \sum_{t=1}^M |\beta_t|^2 \mathbf{p}^\dagger \mathbf{M}^{-1} \mathbf{p} \mathbf{I}_2 \end{cases}$$

and

$$\mathbf{J}_{\boldsymbol{\theta}_\alpha, \boldsymbol{\theta}_p}(\boldsymbol{\theta}) = 2\Re \left(\begin{bmatrix} 1 & j \\ -j & 1 \end{bmatrix} \otimes \mathbf{v}_\xi \otimes \mathbf{p}^\dagger \mathbf{M}^{-1} \right)$$

with $\mathbf{v}_\xi = [\alpha_1, \dots, \alpha_M]^T$ for Scenario 1 and $\mathbf{v}_\xi = \alpha \sum_{t=1}^M |\beta_t|^2$ for Scenario 2.

Additionally, define $\mathbf{f}(\boldsymbol{\theta}) = (\|\mathbf{p}\|^2 - 1, \Im(\mathbf{b}_a^\dagger \mathbf{p}))^T$, and consider the gradient vector of the constraints [21]

$$\mathbf{F}(\boldsymbol{\theta}) = \frac{\partial \mathbf{f}(\boldsymbol{\theta})}{\partial \boldsymbol{\theta}^T} = \begin{cases} \begin{bmatrix} 2\boldsymbol{\theta}_p^T & \mathbf{0}_{2M}^T \\ \check{\mathbf{b}}_a^T & \mathbf{0}_{2M}^T \end{bmatrix} & \text{Scenario 1} \\ \begin{bmatrix} 2\boldsymbol{\theta}_p^T & \mathbf{0}_2^T \\ \check{\mathbf{b}}_a^T & \mathbf{0}_2^T \end{bmatrix} & \text{Scenario 2} \end{cases}$$

with $\check{\mathbf{b}}_a = [\Im(\mathbf{b}_a)^T, \Re(\mathbf{b}_a)^T]^T$. The above matrix has a full row rank if $\boldsymbol{\theta}_p$ and $\check{\mathbf{b}}_a$ are not proportional. Focusing on situations where such assumption is satisfied, there exists a matrix \mathbf{U}_c such that (see the equation at the bottom of the page). Hence, by [21, Th. 1], the error covariance \mathbf{C}_θ of an unbiased estimate of $\boldsymbol{\theta}$ complies with

$$\mathbf{C}_\theta \succeq \mathbf{U}_c (\mathbf{U}_c^T \mathbf{J}(\boldsymbol{\theta}) \mathbf{U}_c)^{-1} \mathbf{U}_c^T$$

for all $\boldsymbol{\theta}$ such that $\det(\mathbf{U}_c^T \mathbf{J}(\boldsymbol{\theta}) \mathbf{U}_c) \neq 0$. As a byproduct, the error covariance of an unbiased estimate of $\boldsymbol{\theta}_p$ fulfills

$$\mathbf{C}_{\boldsymbol{\theta}_p} \succeq [\mathbf{U}_c (\mathbf{U}_c^T \mathbf{J}(\boldsymbol{\theta}) \mathbf{U}_c)^{-1} \mathbf{U}_c^T]_{\boldsymbol{\theta}_p, \boldsymbol{\theta}_p} \quad (23)$$

with $[\mathbf{U}_c (\mathbf{U}_c^T \mathbf{J}(\boldsymbol{\theta}) \mathbf{U}_c)^{-1} \mathbf{U}_c^T]_{\boldsymbol{\theta}_p, \boldsymbol{\theta}_p}$ the matrix formed by the first $2N$ rows and $2N$ columns of $\mathbf{U}_c (\mathbf{U}_c^T \mathbf{J}(\boldsymbol{\theta}) \mathbf{U}_c)^{-1} \mathbf{U}_c^T$.

Example: In this example, we study the mean square error (MSE) of the proposed algorithm, i.e.

$$\text{MSE} = \frac{1}{N_{\text{trials}}} \sum_{t=1}^{N_{\text{trials}}} \|\mathbf{p}_{\text{ML}}^{(t)} - \mathbf{p}\|^2 \quad (24)$$

(where N_{trials} denotes the number of independent data realizations used to perform the MSE estimate and $\mathbf{p}_{\text{ML}}^{(t)}$ is the t th ML estimate of \mathbf{p}) in comparison with the trace of the CRB matrix [right-hand side (RHS) of (23)]. To this end, we assume $N = 5$, $M = 25$, covariance disturbance exponentially shaped with one-lag coefficient $\rho = 0.9$, elliptical constraint with $\mathbf{E} = \mathbf{I}/\epsilon$, $\mathbf{p} = \mathbf{p}_0 = 1/N[1, \dots, 1]^T$. The convex optimization MATLAB toolbox SElf-DUal-MInimization (SeDuMi) [35] is exploited for solving the SDP problem involved in Algorithm 1.⁹

In Fig. 2, MSE is plotted versus the signal-to-noise ratio (SNR), i.e.

$$\text{SNR} = \sum_{t=1}^M |\alpha_t|^2 \mathbf{p}_0^\dagger \mathbf{M}^{-1} \mathbf{p}_0 \quad (25)$$

for $N_{\text{trials}} = 1000$ and several values of the parameter ϵ . We observe that, as the SNR increases, the method's MSE approaches the trace of the constrained CRB matrix. Additionally, the lower

⁹The same solver is also exploited in the remaining simulations of the paper.

$$\mathbf{U}_c \mathbf{U}_c^T = \left(\mathbf{I}_{2(N+M)} - \mathbf{F}^T(\boldsymbol{\theta}) (\mathbf{F}(\boldsymbol{\theta}) \mathbf{F}^T(\boldsymbol{\theta}))^{-1} \mathbf{F}(\boldsymbol{\theta}) \right), \quad \mathbf{U}_c^T \mathbf{U}_c = \mathbf{I}_{2(N+M)-1} \quad \text{Scenario 1}$$

$$\mathbf{U}_c \mathbf{U}_c^T = \left(\mathbf{I}_{2(N+1)} - \mathbf{F}^T(\boldsymbol{\theta}) (\mathbf{F}(\boldsymbol{\theta}) \mathbf{F}^T(\boldsymbol{\theta}))^{-1} \mathbf{F}(\boldsymbol{\theta}) \right), \quad \mathbf{U}_c^T \mathbf{U}_c = \mathbf{I}_{2(N+1)-1} \quad \text{Scenario 2.}$$

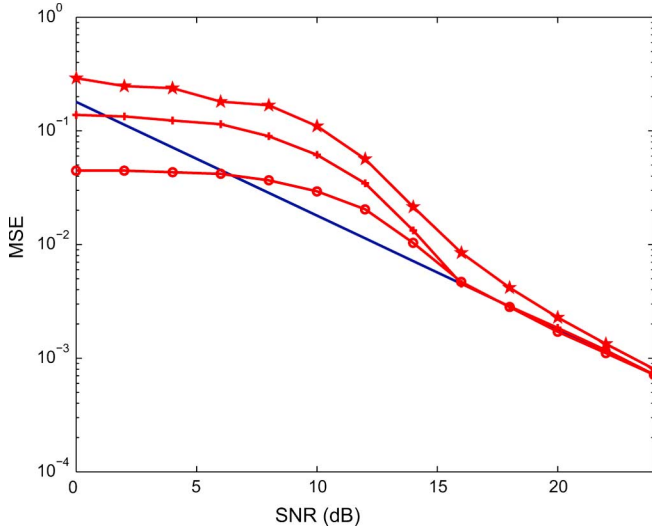


Fig. 2. MSE versus SNR for $N = 5$, $M = 25$, perfectly matched steering direction, and several values of ϵ . Trace of the constrained CRB matrix [RHS of (23)] solid line. $\epsilon = 0.05$ o-marked curve. $\epsilon = 0.1$ + -marked curve. $\epsilon = 2$ star-marked curve.

the uncertainty (in this case the volume of the ellipsoid around the true steering direction), the better the performance.

IV. APPLICATIONS

In this section, we present two applications of the estimation technique developed in the previous section. Precisely, we will focus on the problems of radar detection of range distributed targets with an elliptical steering constraint and robust point-target detection with a radar using a general antenna array configuration with a mix of high- and low-gain beams.

A. Detection of Range Distributed Targets With an Elliptical Steering Constraint

Assume that data are collected by an array of N sensors and deal with the problem of detecting the presence of a target across M range cells ($M \geq N$). Let \mathbf{z}_t , $t = 1, \dots, M$, be the N -dimensional vector of the received signal from the t -th range cell (primary data). Assume that a secondary data set, \mathbf{z}_t , $t = M+1, \dots, K$, is available and each of such snapshots does not contain any useful target echo.

The detection problem to be solved can be formulated in terms of the following binary hypotheses test:

$$\begin{cases} H_0 : \mathbf{z}_t = \mathbf{n}_t, & t = 1, \dots, K \\ H_1 : \begin{cases} \mathbf{z}_t = \alpha_t \mathbf{p} + \mathbf{n}_t, & t = 1, \dots, M \\ \mathbf{z}_t = \mathbf{n}_t, & t = M+1, \dots, K \end{cases} \end{cases} \quad (26)$$

where

- α_t 's are unknown parameters accounting for the useful target reflectivity and channel propagation effects;
- \mathbf{n}_t 's are N -dimensional disturbance vectors modeled as independent, zero-mean, complex Gaussian vectors with the same unknown covariance matrix, i.e.

$$E[\mathbf{n}_t \mathbf{n}_t^\dagger] = \mathbf{M}, t = 1, \dots, K;$$

- \mathbf{p} is the actual steering vector, which due to several effects might not be aligned with the nominal steering \mathbf{s} . In particular, in this application, we suppose that \mathbf{p} belongs to the set $\Omega = \mathcal{U} \cap \mathcal{C}$ where $\mathcal{C} = \left\{ \mathbf{p} \in \mathbb{C}^N : (\mathbf{p} - \mathbf{p}_0)^\dagger \mathbf{E}(\mathbf{p} - \mathbf{p}_0) \leq 1 \right\}$, and \mathbf{E} is a positive definite (or possibly semidefinite) matrix.

We investigate three possible statistical tests for the hypotheses test (26), i.e., the one-step generalized likelihood ratio test (GLRT), the two-step GLRT, and the modified two-step GLRT, which in the absence of steering mismatches have been derived in [14].

One-Step GLRT: The one-step GLRT is the following decision rule shown in (27) at the bottom of the page, where $f(\mathbf{z}_1, \dots, \mathbf{z}_K | H_1, \alpha_1, \dots, \alpha_M, \mathbf{p}, \mathbf{M})$ and $f(\mathbf{z}_1, \dots, \mathbf{z}_K | H_0, \mathbf{M})$, are the data pdf's under H_1 and H_0 , respectively, and T is the detection threshold set according to a design false alarm Probability (P_{fa}). Performing the maximizations over \mathbf{M} , $\alpha_1, \dots, \alpha_M$, after some standard algebra, we obtain the following decision rule:

$$\max_{\mathbf{p} \in \Omega} \frac{\mathbf{p}^\dagger \mathbf{S}_s^{-1} \mathbf{Z} (\mathbf{I} + \mathbf{Z}^\dagger \mathbf{S}_s^{-1} \mathbf{Z})^{-1} \mathbf{Z}^\dagger \mathbf{S}_s^{-1} \mathbf{p}}{\mathbf{p}^\dagger \mathbf{S}_s^{-1} \mathbf{p}} \underset{H_0}{\overset{H_1}{\geq}} T \quad (28)$$

where $\mathbf{Z} = [\mathbf{z}_1, \dots, \mathbf{z}_M]$, $\mathbf{S}_s = \sum_{t=M+1}^K \mathbf{z}_t \mathbf{z}_t^\dagger$, and the same symbol T has been used to denote the modified threshold. Evidently, the optimization problem involved in the computation of the decision statistic can be solved resorting to the framework developed in the previous section based on the Charnes-Cooper transformation.

Two-Step GLRT: This two-step procedure first derives the GLRT based on primary data, assuming that the covariance matrix is known (step 1). Then, a fully adaptive detector is obtained by substituting the unknown matrix with the sample covariance matrix based on secondary data only (step 2). Step 1 can be accomplished evaluating

$$\max_{\mathbf{p} \in \Omega} \max_{\alpha_1, \dots, \alpha_M} \frac{f(\mathbf{z}_1, \dots, \mathbf{z}_M | H_1, \alpha_1, \dots, \alpha_M, \mathbf{p}, \mathbf{M})}{f(\mathbf{z}_1, \dots, \mathbf{z}_M | H_0, \mathbf{M})} \underset{H_0}{\overset{H_1}{\geq}} T \quad (29)$$

$$\max_{\mathbf{p} \in \Omega} \max_{\alpha_1, \dots, \alpha_M} \max_{\mathbf{M}} \frac{f(\mathbf{z}_1, \dots, \mathbf{z}_K | H_1, \alpha_1, \dots, \alpha_M, \mathbf{p}, \mathbf{M})}{\max_{\mathbf{M}} f(\mathbf{z}_1, \dots, \mathbf{z}_K | H_0, \mathbf{M})} \underset{H_0}{\overset{H_1}{\geq}} T \quad (27)$$

which, after some algebra leads to

$$\max_{\mathbf{p} \in \Omega} \frac{\mathbf{p}^\dagger \mathbf{M}^{-1} \mathbf{Z} \mathbf{Z}^\dagger \mathbf{M}^{-1} \mathbf{p}}{\mathbf{p}^\dagger \mathbf{M}^{-1} \mathbf{p}} \underset{H_0}{\overset{H_1}{\geq}} T. \quad (30)$$

Hence, a completely adaptive detector (step 2) can be obtained plugging \mathbf{S}_s in place of \mathbf{M} , i.e.,

$$\max_{\mathbf{p} \in \Omega} \frac{\mathbf{p}^\dagger \mathbf{S}_s^{-1} \mathbf{Z} \mathbf{Z}^\dagger \mathbf{S}_s^{-1} \mathbf{p}}{\mathbf{p}^\dagger \mathbf{S}_s^{-1} \mathbf{p}} \underset{H_0}{\overset{H_1}{\geq}} T. \quad (31)$$

The last maximization can be performed with the procedure of Section II.

Modified Two-Step GLRT: This modified two-step procedure first derives the GLRT based on primary data, assuming that the covariance structure Σ ($\mathbf{M} = \sigma^2 \Sigma$) is known (step 1). Then, a fully adaptive detector is obtained by substituting the sample covariance matrix in place of Σ (step 2).

Step 1 requires the computation of (32) at the bottom of the page, which, after some algebra, can be recast as

$$\max_{\mathbf{p} \in \Omega} \frac{\mathbf{p}^\dagger \Sigma^{-1} \mathbf{Z} \mathbf{Z}^\dagger \Sigma^{-1} \mathbf{p}}{\text{tr}(\mathbf{Z}^\dagger \Sigma^{-1} \mathbf{Z}) \mathbf{p}^\dagger \Sigma^{-1} \mathbf{p}} \underset{H_0}{\overset{H_1}{\geq}} T. \quad (33)$$

Plugging \mathbf{S}_s in place of Σ , we get the modified two-step GLRT, i.e.

$$\max_{\mathbf{p} \in \Omega} \frac{\mathbf{p}^\dagger \mathbf{S}_s^{-1} \mathbf{Z} \mathbf{Z}^\dagger \mathbf{S}_s^{-1} \mathbf{p}}{\text{tr}(\mathbf{Z}^\dagger \mathbf{S}_s^{-1} \mathbf{Z}) \mathbf{p}^\dagger \Sigma^{-1} \mathbf{p}} \underset{H_0}{\overset{H_1}{\geq}} T. \quad (34)$$

Again, Algorithm 1 of Section II can be used to obtain the optimal value of the maximization problem in (34).

The new detectors (28), (31), and (34), will be respectively referred to as Elliptically Constrained One-Step GLRT (EC-1S-GLRT), EC Two-Step GLRT (EC-2S-GLRT), and EC Modified 2S-GLRT (EC-M2S-GLRT). Their counterparts, derived in [14] and assuming the perfect knowledge of \mathbf{p} , are instead respectively referred to as 1S-GLRT, 2S-GLRT, and M2S-GLRT.

In the following, we analyze the performance of the six considered receivers assuming $N = 5$, $K = 15$, $M = 3$, target uniformly spread within the M range cells, covariance disturbance exponentially shaped with one-lag coefficient $\rho = 0.9$, false alarm probability $P_{fa} = 10^{-2}$, $\mathbf{E} = \mathbf{I}/\epsilon$, and $\epsilon = 0.1$. As to the actual steering direction \mathbf{p} , we simulate it as follows:

$$\mathbf{p} = \mathbf{p}_0 \cos \theta_m + \mathbf{p}_0^\perp \sin \theta_m$$

where \mathbf{p}_0^\perp denotes a (random) unit norm vector orthogonal to the nominal direction \mathbf{p}_0 and θ_m is a parameter which rules the degree of mismatch.

In Fig. 3(a), we plot the detection Probability P_d (evaluated through Monte Carlo techniques) versus SNR (25) for $\theta_m =$

0, namely actual steering direction perfectly matched with the nominal one. The curves show that the receivers which know exactly the steering direction outperform the elliptically constrained detectors which assume some uncertainty on the actual steering direction. Indeed, for $P_d = 0.9$, the detection loss is always kept within 4 dB for all the three considered design strategies.

In Fig. 3(b), we consider the case where some mismatch is present. Precisely, we set $\theta_m = \text{asin}(\sqrt{\epsilon}/2)$. Evidently, the classic receivers show a performance degradation which might also be severe for the cases of the 1S-GLRT and the M2S-GLRT. As to the elliptically constrained receivers, they exhibit a more robust behavior with respect to directional mismatches thanks to the uncertainty on the steering direction that they suppose at the design stage.

Finally, in Fig. 3(c), we analyze the effect of the parameter ϵ on the detection performance for $\theta_m = 0$. The plots show that the higher ϵ the higher the loss of each elliptically constrained receiver with respect to its counterpart which exactly knows the steering direction. This behavior can be explained observing that the higher ϵ the wider the uncertainty region where the actual steering vector is supposed to belong to. Additionally, it seems that the EC-M2S-GLRT is the most sensitive among the new receivers, whereas the EC-1S-GLRT and EC-2S-GLRT exhibit almost the same degree of sensitivity.

B. Robust Point-Target Detection With a Radar Using a General Antenna Array Configuration With a Mix of High- and Low-Gain Beams

Let us consider a radar operating with a general antenna array configuration [17] which includes a mix of high- and low-gain beams, obtained by suitable linear combinations of basic array elements. The radar is equipped with N independent receiving channels, each connected with one of the beams. According to the model developed in [17], the echoes collected by the N channels at the t th sampling instant are stacked to form the N -dimensional vector \mathbf{z}_t , $t = 0, \dots, K$ ($K + 1 \geq N$), referred to as t -th snapshot (for notational simplicity we assume that \mathbf{z}_0 contains the echo from the cell under test). As to the spatial behavior of the expected target, it is described by the N -dimensional steering vector \mathbf{p}_θ whose components are the complex amplitudes of the echo received at the N -th channel from a normalized target with direction of arrival θ . If the radar contains P high-gain beams then $\mathbf{p}_\theta = [\mathbf{p}^T, \mathbf{0}]^T$ (\mathbf{p} is a P -dimensional column vector), since the usual signal received at the low-gain beams can be considered with a negligible power level [17].

The temporal behavior of the expected target echo is described by the $(K + 1)$ -dimensional vector $\mathbf{s} = [s_0, s_1, \dots, s_{K+1}]^T$ corresponding to the samples of the coded transmitted waveform (assumed, without loss of generality, with unit norm). Finally, the global disturbance is a combination of thermal noise and narrowband directional jam-

$$\frac{\max_{\mathbf{p} \in \Omega} \max_{\alpha_1, \dots, \alpha_M} \max_{\sigma^2} f(\mathbf{z}_1, \dots, \mathbf{z}_M | H_1, \alpha_1, \dots, \alpha_M, \mathbf{p}, \sigma^2, \Sigma)}{\max_{\sigma^2} f(\mathbf{z}_1, \dots, \mathbf{z}_M | H_0, \sigma^2, \Sigma)} \underset{H_0}{\overset{H_1}{\geq}} T \quad (32)$$

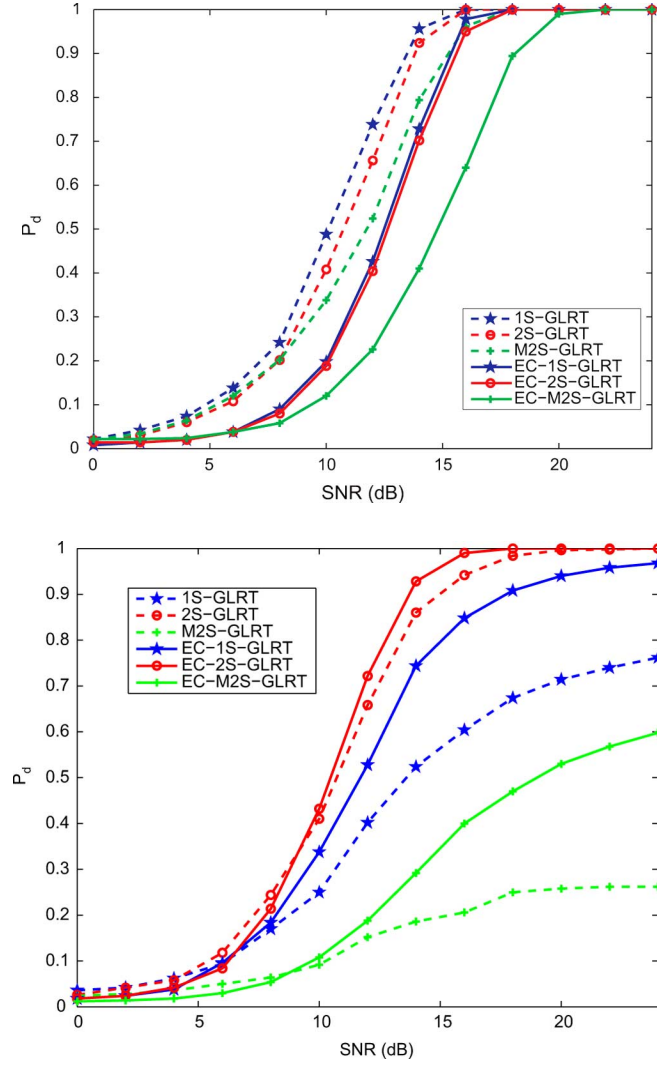


Fig. 3. (a) P_d versus SNR for $P_{fa} = 10^{-2}$, $N = 5$, $K = 15$, $M = 3$, $\epsilon = 0.1$, and perfectly matched steering direction. 1S-GLRT (dashed star-marked curve), 2S-GLRT (dashed o-marked curve), M2S-GLRT (dashed + -marked curve), EC-1S-GLRT (solid star-marked curve), EC-2S-GLRT (solid o-marked curve), EC-M2S-GLRT (solid + -marked curve). (b) P_d versus SNR for $P_{fa} = 10^{-2}$, $N = 5$, $K = 15$, $M = 3$, $\epsilon = 0.1$, mismatched steering direction with $\theta_m = \text{asin}(\sqrt{\epsilon}/2)$. 1S-GLRT (dashed star-marked curve), 2S-GLRT (dashed o-marked curve), M2S-GLRT (dashed + -marked curve), EC-1S-GLRT (solid star-marked curve), EC-2S-GLRT (solid o-marked curve), EC-M2S-GLRT (solid + -marked curve).

mers. Hence, the $(K + 1)$ snapshots are modeled as independent complex Gaussian vectors with unknown covariance matrix \mathbf{M} and mean $\alpha_{S_k} \mathbf{p}_\theta$ under H_1 (0 under H_0) with α an unknown parameter accounting for the target backscattering and channel propagation effects.

Let us denote by

$$\mathbf{Z} = [z_0, \dots, z_K]^T = \begin{bmatrix} \mathbf{Z}_h \\ \mathbf{Z}_l \end{bmatrix}$$

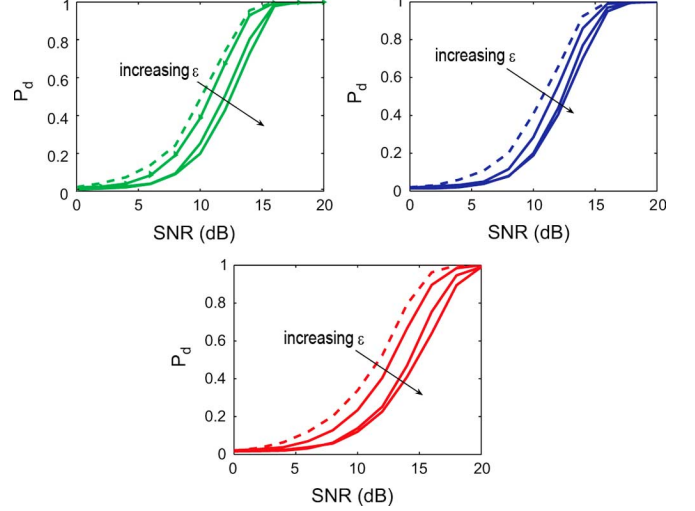


Fig. 3. (Continued.) (c) P_d versus SNR for $P_{fa} = 10^{-2}$, $N = 5$, $K = 15$, $M = 3$, perfectly matched steering direction, and several values of $\epsilon \in \{0.01, 0.05, 0.1\}$. Subplot a) 1S-GLRT (dashed curve) and EC-1S-GLRT (solid curves). Subplot b) 2S-GLRT (dashed curve) and EC-2S-GLRT (solid curves). Subplot c) M2S-GLRT (dashed curve) and EC-M2S-GLRT (solid curves).

where \mathbf{Z}_h is a $P \times (K + 1)$ matrix containing the P high-gain beams of each snapshot. The generalized likelihood ratio (GLR) for known \mathbf{p} can be written as [17]

$$\begin{aligned} & \max_{\alpha, \mathbf{M}} \frac{f(\mathbf{Z} | H_1, \alpha, \mathbf{p}, \mathbf{M})}{\max_{\mathbf{M}} f(\mathbf{Z} | H_0, \mathbf{M})} \\ &= \left[1 - \frac{|\mathbf{p}^\dagger \Phi^{-1} \mathbf{Y}_C \mathbf{s}^*|^2}{(1 + \mathbf{s}^T \mathbf{Z}^\dagger (\mathbf{Z} \mathbf{P}_s \mathbf{Z}^\dagger)^{-1} \mathbf{Z} \mathbf{s}^*) \mathbf{p}^\dagger \Phi^{-1} \mathbf{p}} \right]^{-(K+1)} \end{aligned} \quad (35)$$

where

$$\begin{aligned} \mathbf{P}_s &= \mathbf{I} - \mathbf{s}^* \mathbf{s}^T \\ \Phi &= \mathbf{Z}_h \mathbf{P}_s [\mathbf{I} - \mathbf{P}_s \mathbf{Z}_l^\dagger (\mathbf{Z}_l \mathbf{P}_s \mathbf{Z}_l^\dagger)^{-1} \mathbf{Z}_l \mathbf{P}_s] \mathbf{P}_s \mathbf{Z}_h^\dagger \\ \mathbf{Y}_C &= \mathbf{Z}_h [\mathbf{I} - \mathbf{P}_s \mathbf{Z}_l^\dagger (\mathbf{Z}_l \mathbf{P}_s \mathbf{Z}_l^\dagger)^{-1} \mathbf{Z}_l]. \end{aligned}$$

Assuming that some uncertainty is available on \mathbf{p} , for instance due to array pointing errors or miscalibration effects, one can resort to a further GLR over \mathbf{p} in order to cope with the additional unknown parameter. If an elliptical model, as that of the previous subsection, is considered for the uncertainty region, then the GLR becomes

$$\max_{\mathbf{p} \in \Omega} \left[1 - \frac{|\mathbf{p}^\dagger \Phi^{-1} \mathbf{Y}_C \mathbf{s}^*|^2}{(1 + \mathbf{s}^T \mathbf{Z}^\dagger (\mathbf{Z} \mathbf{P}_s \mathbf{Z}^\dagger)^{-1} \mathbf{Z} \mathbf{s}^*) \mathbf{p}^\dagger \Phi^{-1} \mathbf{p}} \right]^{-(K+1)} \quad (36)$$

which can be equivalently written as shown (37), shown at the bottom of the page. The maximization in (37) can be accomplished through Algorithm 1 of Section II. From the above equation, we can construct the GLRT obtained comparing the GLR

$$\left[1 - \frac{1}{(1 + \mathbf{s}^T \mathbf{Z}^\dagger (\mathbf{Z} \mathbf{P}_s \mathbf{Z}^\dagger)^{-1} \mathbf{Z} \mathbf{s}^*)} \max_{\mathbf{p} \in \Omega} \frac{\mathbf{p}^\dagger \Phi^{-1} \mathbf{Y}_C \mathbf{s}^* \mathbf{s}^T \mathbf{Y}_C^\dagger \Phi^{-1} \mathbf{p}}{\mathbf{p}^\dagger \Phi^{-1} \mathbf{p}} \right]^{-(K+1)}. \quad (37)$$

with a threshold, set in order to ensure the design P_{fa} . The resulting detector will be referred to as the EC-GLRT and is given by

$$\frac{1}{(1 + \mathbf{s}^T \mathbf{Z}^\dagger (\mathbf{Z} \mathbf{P}_s \mathbf{Z}^\dagger)^{-1} \mathbf{Z} \mathbf{s}^*)} \times \max_{\mathbf{p} \in \Omega} \frac{\mathbf{p}^\dagger \Phi^{-1} \mathbf{Y}_C \mathbf{s}^* \mathbf{s}^T \mathbf{Y}_C^\dagger \Phi^{-1} \mathbf{p}}{\mathbf{p}^\dagger \Phi^{-1} \mathbf{p}} \underset{H_0}{\overset{H_1}{\geq}} T. \quad (38)$$

Its counterpart, assuming the perfect knowledge of \mathbf{p} , will be instead referred to as the GLRT. In the following, we assess the performance of the EC-GLRT and the GLRT assuming that the actual steering direction is modeled as¹⁰

$$\alpha \mathbf{p}(i) = \alpha_1 (1 + a(i)) \exp(j\pi \sin(\phi_p + \phi_m(i))) \quad i = 1, \dots, P$$

where $a(i)$ is a sequence of independent zero-mean Gaussian random variables with variance σ_a^2 and $\phi_m(i)$ is another sequence (statistically independent of $a(i)$) of independent zero-mean Gaussian random variables with variance σ_m^2 . As to the disturbance scenario, we suppose the presence of noise plus two jammers impinging from 10 and 20 degrees, respectively, with a jammer to noise ratio of 20 dB.

In Fig. 4(a), we plot P_d (evaluated through Monte Carlo techniques) of the two detectors versus SNR, i.e.

$$\text{SNR} = |\alpha|^2 [\mathbf{p}_0^\dagger, \mathbf{0}^\dagger] \mathbf{M}^{-1} [\mathbf{p}_0^T, \mathbf{0}^T]^T$$

where \mathbf{p}_0 is the nominal direction (i.e., $\mathbf{p}_0(i) = 1/\sqrt{P} \exp(j\pi \sin(\phi_p))$), $i = 1, \dots, P$, for $P_{fa} = 10^{-2}$, $N = 10$, $P = 5$, $K = 12$, $\epsilon = 0.2$, $\phi_p = 0$, $\sigma_a = 0.1$, and two values of σ_m . The transmitted waveform \mathbf{s} is a Barker code of length 13. For comparison purposes, the case of a perfectly matched steering direction is plotted as well.

The analysis of the curves shows that if a useful signal, perfectly matched to the nominal steering direction, impinges on the array, then the EC-GLRT exhibits almost the same P_d as the GLRT and, for $P_d > 0.9$, the respective performance curves overlap. When a mismatch is present, the EC-GLRT achieves a performance level better than the GLRT; specifically the stronger the mismatch the higher the detection gain.

The effect of the parameter σ_a is analyzed in Fig. 4(b), where P_d is plotted versus SNR for several values of σ_a , $\sigma_m = 3$, and the remaining simulation parameters as in Fig. 4(a). The plots highlight that the performance gain of the EC-GLRT over the GLRT depends on the entity of the amplitude mismatch; precisely, the higher the amplitude mismatch the higher the gain of the receiver which compensates for the amplitude mismatch. Summarizing, both the figures are a confirmation that, the elliptically constrained receiver is more robust than the counterpart with respect to directional mismatches.

V. CONCLUSION

In this paper, we have considered the problem of constrained steering direction estimation of a signal embedded in Gaussian disturbance. The constraint set has been represented in terms of a general quadratic inequality constraint which includes

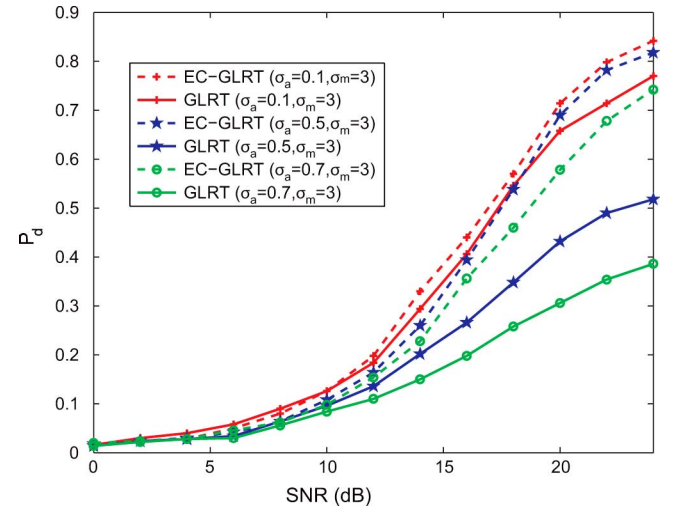
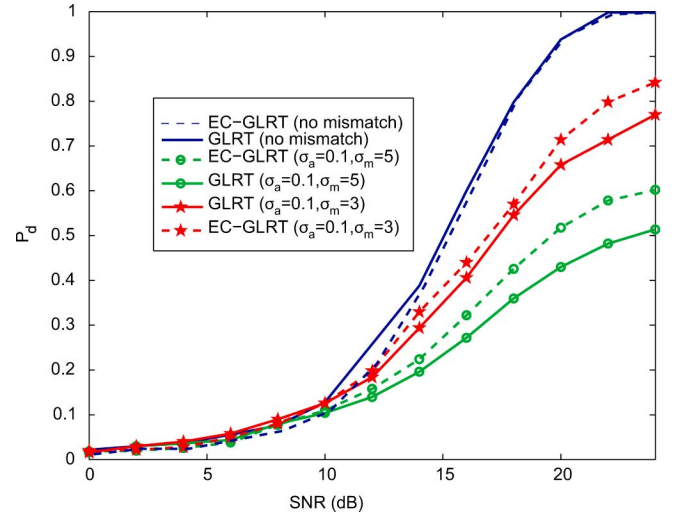


Fig. 4. (a) P_d versus SNR for $P_{fa} = 10^{-2}$, $N = 10$, $P = 5$, $K = 12$, $\epsilon = 0.2$, mismatched steering direction with $\sigma_a = 0.1$ and two values of σ_m ($\sigma_m = 3$ star-marked curves and $\sigma_m = 5$ o-marked curves), GLRT (solid curves), EC-GLRT (dashed curves). (b) P_d versus SNR for $P_{fa} = 10^{-2}$, $N = 10$, $P = 5$, $K = 12$, $\epsilon = 0.2$, mismatched steering direction with $\sigma_m = 3$ and three values of σ_a ($\sigma_a = 0.1$ +-marked curves), $\sigma_a = 0.5$ star-marked curves, and $\sigma_a = 0.7$ o-marked curves.

many situations of practical relevance such as conic constraints, elliptical constraints, exterior conic constraints, and exterior elliptical constraints. Additionally, a norm constraint accounting for the unitary norm of the steering direction has been considered. The estimation problem is attacked resorting to the ML criterion under two different assumptions for the received signal amplitude:

- the complex amplitude of the useful signal component changes from snapshot to snapshot;
- the useful signal keeps a constant amplitude within all the snapshots.

We have proved that the ML criterion leads in both cases to a fractional QCQP. In order to solve it, we have first relaxed the problem into a constrained fractional SDP problem which we prove equivalent to an SDP problem through the Charnes-Cooper transformation. Then, exploiting some rank-one decompositions, we have shown that the SDP relaxation is actually

¹⁰We are accounting for both amplitude and phase mismatch.

tight. Additionally, we have devised a procedure which constructs (in polynomial time) an optimal solution of the original problem from an optimal solution of the fractional SDP. We have also analyzed the quality of the derived estimator through a comparison of its performance with the constrained CRB. Finally, we have given two applications of the proposed theoretical framework in the context of radar detection of range distributed targets and robust point-target detection with a radar using a general antenna array configuration with a mix of high- and low-gain beams. In both the situations, the new procedure applies successfully.

Possible future research tracks might concern the application of the framework to additional statistical signal processing problems involving over the horizon (OTH) radar or synthetic aperture radar (SAR) processing (including atmospheric effects) as well as the extension of the procedure to account for the presence of a specific structure in the steering direction.

APPENDIX

A. Proof of Lemma 3.1

Proof: Observe that the feasible region of \mathcal{P}_3

$$\Omega' = \{\mathbf{W} \succeq \mathbf{0} | \text{tr}(\mathbf{Q}_1 \mathbf{W}) \geq 0, \text{tr}(\mathbf{Q}_2 \mathbf{W}) = 1, \text{tr}(\mathbf{Q}_3 \mathbf{W}) = 1\} \quad (39)$$

is a closed subset of the compact set

$$\Omega'' = \{\mathbf{W} \succeq \mathbf{0} | \text{tr}((\mathbf{Q}_2 + \mathbf{Q}_3) \mathbf{W}) = \text{tr}(\mathbf{W}) = 2\}$$

thus the set Ω' is compact as well. Also note that the denominator and numerator of the objective function of the fractional SDP \mathcal{P}_3 are continuous, and that the denominator is positive over the feasible region (because $\text{tr}(\mathbf{Q}_0 \mathbf{W}) > 0$ for any \mathbf{W} belonging to the set $\{\mathbf{W} \succeq \mathbf{0} | \text{tr}(\mathbf{Q}_2 \mathbf{W}) = 1\}$ which includes the feasible region). Let $\Omega''' = \{\mathbf{W} \succeq \mathbf{0} | \text{tr}(\mathbf{Q}_2 \mathbf{W}) = 1\}$. Then, for any $\mathbf{W} \in \Omega'$, we have that

$$\begin{aligned} 0 &\leq \text{tr}(\mathbf{Q}_{-1} \mathbf{W}) \leq \underset{\mathbf{Y} \in \Omega'''}{\text{maximize}} \text{tr}(\mathbf{Q}_{-1} \mathbf{Y}) \\ &= \lambda_{\max}(\mathbf{M}^{-1} \mathbf{S} \mathbf{M}^{-1}) \end{aligned}$$

and

$$\begin{aligned} \lambda_{\min}(\mathbf{M}^{-1}) &= \underset{\mathbf{Y} \in \Omega'''}{\text{minimize}} \text{tr}(\mathbf{Q}_0 \mathbf{Y}) \leq \text{tr}(\mathbf{Q}_0 \mathbf{W}) \\ &\leq \underset{\mathbf{Y} \in \Omega'''}{\text{maximize}} \text{tr}(\mathbf{Q}_0 \mathbf{Y}) = \lambda_{\max}(\mathbf{M}^{-1}). \end{aligned}$$

This implies that the objective function of problem \mathcal{P}_3 is finite-valued over the feasible region. It follows from Weierstrass' Theorem (for instance, see [36, Ch. 2]) that problem \mathcal{P}_3 has always an optimal solution. Hence, the problem is solvable. ■

B. Proof of Lemma 3.2

Proof: The dual of SDP \mathcal{P}_4 is shown in

$$\mathcal{P}_d \begin{cases} \underset{y_0, y_1, y_2, y_3}{\text{minimize}} & y_0 \\ \text{subject to} & \mathbf{Q}_{-1} - y_0 \mathbf{Q}_0 - y_1 \mathbf{Q}_1 - y_2 \mathbf{Q}_2 - y_3 \mathbf{Q}_3 \preceq \mathbf{0} \\ & y_2 + y_3 \leq 0 \\ & y_1 \leq 0. \end{cases} \quad (40)$$

Since \mathcal{P}_3 has an optimal solution, say \mathbf{W}^* , hence it is easily seen that $(\mathbf{W}^*/\text{tr}(\mathbf{Q}_0 \mathbf{W}^*), 1/\text{tr}(\mathbf{Q}_0 \mathbf{W}^*))$ is feasible for \mathcal{P}_d . Therefore, by weak duality, Problem \mathcal{P}_d is bounded below. Assume

that $y_1 = \epsilon_1 < 0$ and $y_2 = \epsilon_2 < 0$ are given such that $\epsilon_2 - \epsilon_1 c < 0$. Then see,

$$\begin{aligned} \mathbf{Q}_{-1} - y_0 \mathbf{Q}_0 - y_1 \mathbf{Q}_1 - y_2 \mathbf{Q}_2 - y_3 \mathbf{Q}_3 = \\ \begin{bmatrix} \mathbf{M}^{-1} \mathbf{S} \mathbf{M}^{-1} - y_0 \mathbf{M}^{-1} - \epsilon_1 \mathbf{A} - \epsilon_2 \mathbf{I} & -\epsilon_1 \mathbf{b} \\ -\epsilon_1 \mathbf{b}^\dagger & -\epsilon_1 c - y_3 \end{bmatrix} \preceq \mathbf{0} \end{aligned}$$

which is equivalent to

$$\begin{bmatrix} y_0 \mathbf{M}^{-1} + \epsilon_1 \mathbf{A} + \epsilon_2 \mathbf{I} - \mathbf{M}^{-1} \mathbf{S} \mathbf{M}^{-1} & \epsilon_1 \mathbf{b} \\ \epsilon_1 \mathbf{b}^\dagger & \epsilon_1 c + y_3 \end{bmatrix} \succeq \mathbf{0}.$$

Now, we can set $y_0 > 0$ to be sufficiently large and set y_3 so that $\epsilon_1^2 \mathbf{b}^\dagger (y_0 \mathbf{M}^{-1} + \epsilon_1 \mathbf{A} + \epsilon_2 \mathbf{I} - \mathbf{M}^{-1} \mathbf{S} \mathbf{M}^{-1})^{-1} \mathbf{b}$ is close enough to zero, and $y_3 > \epsilon_1^2 \mathbf{b}^\dagger (y_0 \mathbf{M}^{-1} + \epsilon_1 \mathbf{A} + \epsilon_2 \mathbf{I} - \mathbf{M}^{-1} \mathbf{S} \mathbf{M}^{-1})^{-1} \mathbf{b} - \epsilon_1 c$ and $y_3 + y_2 = y_3 + \epsilon_2 < 0$. This means the SDP problem \mathcal{P}_d is strictly feasible. It follows from the strong duality theorem (for example, see [32, Th. 1.7.1]) that Problem \mathcal{P}_4 is solvable. ■

C. Proof of Lemma 3.3

Proof: Suppose that \mathbf{W}^* is an optimal solution of \mathcal{P}_3 and $v(\mathcal{P}_3)$ is the optimal value of \mathcal{P}_3 , and that $v(\mathcal{P}_4)$ is the optimal value of \mathcal{P}_4 . It is verified easily that $(\mathbf{W}^*/\text{tr}(\mathbf{Q}_0 \mathbf{W}^*), s^*)$ with $s^* = 1/\text{tr}(\mathbf{Q}_0 \mathbf{W}^*)$ is feasible for \mathcal{P}_4 , and the objective function value at the feasible point is $\text{tr}(\mathbf{Q}_{-1} \mathbf{W}^*)/\text{tr}(\mathbf{Q}_0 \mathbf{W}^*) = v(\mathcal{P}_3)$. Thus, we have $v(\mathcal{P}_4) \geq v(\mathcal{P}_3)$.

On the other hand, let (\mathbf{X}^*, s^*) be an optimal solution of \mathcal{P}_4 . We claim that $s^* > 0$. Indeed, if $s^* = 0$, then $\text{tr}(\mathbf{Q}_2 \mathbf{X}^*) + \text{tr}(\mathbf{Q}_3 \mathbf{X}^*) = \text{tr}(\mathbf{X}^*) = 2s^* = 0$, which implies $\mathbf{X}^* = \mathbf{0}$. This is impossible since $\text{tr}(\mathbf{Q}_0 \mathbf{X}^*) = 1$. It is checked that \mathbf{X}^*/s^* is feasible for \mathcal{P}_3 , and the objective function value of \mathcal{P}_3 at the feasible point is $\text{tr}(\mathbf{Q}_{-1} (\mathbf{X}^*/s^*)) / \text{tr}(\mathbf{Q}_0 (\mathbf{X}^*/s^*)) = \text{tr}(\mathbf{Q}_{-1} \mathbf{X}^*) / \text{tr}(\mathbf{Q}_0 \mathbf{X}^*) = \text{tr}(\mathbf{Q}_{-1} \mathbf{X}^*) = v(\mathcal{P}_4)$. Therefore, we have $v(\mathcal{P}_3) \geq v(\mathcal{P}_4)$, which yields $v(\mathcal{P}_3) = v(\mathcal{P}_4)$. ■

ACKNOWLEDGMENT

The authors thank the Associate Editor and the Reviewers for their constructive comments toward the improvement of the original submitted paper.

REFERENCES

- [1] S. A. Vorobyov, A. B. Gershman, and Z. Luo, "Robust adaptive beamforming using worst-case performance optimization: A solution to the signal mismatch problem," *IEEE Trans. Signal Process.*, vol. 51, no. 2, pp. 313–324, Feb. 2003.
- [2] P. Stoica, Z. Wang, and J. Li, "Robust Capon beamforming," *IEEE Signal Process. Lett.*, vol. 10, no. 6, pp. 172–175, Jun. 2003.
- [3] J. Li, P. Stoica, and Z. Wang, "On robust Capon beamforming and diagonal loading," *IEEE Trans. Signal Process.*, vol. 51, no. 7, pp. 1702–1715, Jul. 2003.
- [4] J. Li, P. Stoica, and Z. Wang, "Doubly constrained robust Capon beamformer," *IEEE Trans. Signal Process.*, vol. 52, no. 9, pp. 2407–2423, Sep. 2004.
- [5] A. Beck and Y. C. Eldar, "Doubly constrained robust Capon beamformer with ellipsoidal uncertainty sets," *IEEE Trans. Signal Process.*, vol. 55, no. 2, pp. 753–758, Jan. 2007.
- [6] S. Ramprasad, T. W. Parks, and R. Shenoy, "Signal modeling and detection using cone classes," *IEEE Trans. Signal Process.*, vol. 44, no. 2, pp. 329–338, Feb. 1996.
- [7] M. N. Desai and R. S. Mangoubi, "Adaptive robust constrained matched filter and subspace detection," in *Proc. 36th Asilomar Conf. Signals, Syst., Comput.*, Pacific Grove, CA, Nov. 2002, pp. 768–772.
- [8] M. N. Desai and R. S. Mangoubi, "Robust Gaussian and non-Gaussian matched subspace detection," *IEEE Trans. Signal Process.*, vol. 51, no. 12, pp. 3115–3127, Dec. 2003.

- [9] F. Bandiera, A. De Maio, and G. Ricci, "Adaptive CFAR radar detection with conic rejection," *IEEE Trans. Signal Process.*, vol. 55, no. 6, pp. 2533–2541, Jun. 2007.
- [10] O. Besson, "Detection of a signal in linear subspace with bounded mismatch," *IEEE Trans. Aerosp. Electron. Syst.*, vol. 42, no. 3, pp. 1131–1139, Jul. 2006.
- [11] O. Besson, "Adaptive detection with bounded steering vectors mismatch angle," *IEEE Trans. Signal Process.*, vol. 55, no. 4, pp. 1560–1564, Apr. 2007.
- [12] A. De Maio, S. De Nicola, Y. Huang, S. Zhang, and A. Farina, "Adaptive detection and estimation in the presence of useful signal and interference mismatches," *IEEE Trans. Signal Process.*, vol. 57, no. 2, pp. 436–450, Feb. 2009.
- [13] K. Gerlach and M. J. Steiner, "Adaptive detection of range distributed targets," *IEEE Trans. Signal Process.*, vol. 47, no. 7, pp. 1844–1851, Jul. 1999.
- [14] E. Conte, A. De Maio, and G. Ricci, "GLRT-based adaptive detection algorithms for range spread targets," *IEEE Trans. Signal Process.*, vol. 49, no. 7, pp. 1336–1348, Jul. 2001.
- [15] L. Xu, J. Li, and P. Stoica, "Target detection and parameter estimation for MIMO radar systems," *IEEE Trans. Aerosp. Electron. Syst.*, vol. 44, no. 3, pp. 927–939, Jul. 2008.
- [16] J. Li and P. Stoica, *MIMO Radar Signal Processing*. New York: Wiley, 2008.
- [17] A. Farina, P. Lombardo, and L. Ortenzi, "A unified approach to adaptive radar processing with general antenna array configuration," *Signal Process.*, vol. 84, no. 9, pp. 1593–1623, Sep. 2004.
- [18] A. Charnes and W. W. Cooper, "Programming with linear fractional functionals," *Naval Res. Logist. Quarter.*, vol. 9, pp. 181–186, 1962.
- [19] W. Ai, Y. Huang, and S. Zhang, "Further results on rank-one matrix decomposition and its applications," *Math. Program.*, 2009, to be published.
- [20] Y. Huang and S. Zhang, "Complex matrix decomposition and quadratic programming," *Math. Operat. Res.*, vol. 32, no. 3, pp. 758–768, Aug. 2007.
- [21] P. Stoica and B. C. Ng, "On the Cramér-Rao bound under parametric constraints," *IEEE Signal Process. Lett.*, vol. 5, no. 7, pp. 177–179, 1998.
- [22] W.-K. Ma, T. N. Davidson, K. M. Wong, Z.-Q. Luo, and P. C. Ching, "Quasi-maximum-likelihood multiuser detection using semi-definite relaxation with applications to synchronous CDMA," *IEEE Trans. Signal Process.*, vol. 50, no. 4, pp. 912–922, Apr. 2002.
- [23] Y. Yang, C. Zhao, P. Zhou, and W. Xu, "MIMO detection of 16-QAM signaling based on semidefinite relaxation," *IEEE Signal Process. Lett.*, vol. 14, no. 11, pp. 797–800, Nov. 2007.
- [24] N. D. Sidiropoulos and Z.-Q. Luo, "A semidefinite relaxation approach to MIMO detection for high-order QAM constellations," *IEEE Signal Process. Lett.*, vol. 13, no. 9, pp. 525–528, Sep. 2006.
- [25] J. Li, J. R. Guerci, and L. Xu, "Signal waveform's optimal-under-restriction design for active sensing," *IEEE Signal Process. Lett.*, vol. 13, no. 9, pp. 565–568, Sep. 2006.
- [26] R. G. Lorentz and S. Boyd, "Robust minimum variance beamforming," *IEEE Trans. Signal Process.*, vol. 53, no. 5, pp. 1684–1696, May 2005.
- [27] N. B. Pulsone and C. M. Rader, "Adaptive beamformer orthogonal rejection test," *IEEE Trans. Signal Process.*, vol. 49, no. 3, pp. 521–529, Mar. 2001.
- [28] F. Bandiera, D. Orlando, and G. Ricci, "Advanced radar detection schemes under mismatched signal models," in *Synthesis Lectures on Signal Processing N. 8*. New York: Morgan and Claypool, 2009.
- [29] J. P. Crouzeix and J. A. Ferland, "Algorithms for generalized fractional programming," *Math. Program.*, vol. 52, pp. 191–207, 1991.
- [30] A. I. Barros, J. B. G. Frenk, S. Schaible, and S. Zhang, "A new algorithm for generalized fractional programs," *Math. Program.*, vol. 72, pp. 147–175, 1996.
- [31] S. Boyd and L. Vandenberghe, *Convex Optimization*. New York: Cambridge Univ. Press, 2008.
- [32] A. Nemirovski, *Lectures on Modern Convex Optimization, Class Notes*. Atlanta, GA: Georgia Inst. Technol., 2005.
- [33] J. D. Gorman and A. O. Hero, "Lower bounds for parametric estimation with constraints," *IEEE Trans. Inf. Theory*, vol. 26, pp. 1285–2301, Nov. 1990.
- [34] S. M. Kay, *Fundamentals of Statistical Signal Processing: Estimation Theory*. Upper Saddle River, NJ: Prentice-Hall, 1993, vol. 1.
- [35] J. F. Sturm, "Using SeDuMi 1.02, a MATLAB toolbox for optimization over symmetric cones," *Optimization Methods Softw.*, vol. 11–12, pp. 625–653, Aug. 1999.
- [36] D. P. Bertsekas, A. Nedic, and A. E. Ozdaglar, *Convex Analysis and Optimization*. New York: Athena Scientific, 2003.



Antonio De Maio (S'01–A'02–M'03–SM'07) was born in Sorrento, Italy, on June 20, 1974. He received the Dr.Eng. degree (with honors) and the Ph.D. degree in information engineering, both from the University of Naples Federico II, Naples, Italy, in 1998 and 2002, respectively.

From October to December 2004, he was a Visiting Researcher with the U.S. Air Force Research Laboratory, Rome, NY. From November to December 2007, he was a Visiting Researcher with the Chinese University of Hong Kong, Hong Kong. Currently, he is an

Associate Professor with the University of Naples Federico II. His research interest lies in the field of statistical signal processing, with emphasis on radar detection, optimization theory applied to radar signal processing, and multiple-access communications.

Dr. De Maio is the recipient of the 2010 IEEE Fred Nathanson Memorial Award as the young (less than 40 years of age) AESR Radar Engineer 2010 whose performance is particularly noteworthy as evidenced by contributions to the radar art over a period of several years, with the following citation for "robust CFAR detection, knowledge-based radar signal processing, and waveform design and diversity."



Yongwei Huang (M'09) received the B.Sc. degree in computational mathematics in 1998, and the M.Sc. degree in operations research in 2000, both from Chongqing University. In 2005, he received the Ph.D. degree in operations research from the Chinese University of Hong Kong, Hong Kong.

He was a Postdoctoral Fellow with the Department of Systems Engineering and Engineering Management, Chinese University of Hong Kong, and a Visiting Researcher with the Department of Biomedical, Electronic, and Telecommunication Engineering, University of Napoli "Federico II", Italy. Currently, he is a Research Associate with the Department of Electronic and Computer Engineering, Hong Kong University of Science and Technology. His research interests are related to optimization theory and algorithms, including conic optimization, robust optimization, combinatorial optimization, and stochastic optimization, and their applications in signal processing for radar and wireless communications.

Associate with the Department of Electronic and Computer Engineering, Hong Kong University of Science and Technology. His research interests are related to optimization theory and algorithms, including conic optimization, robust optimization, combinatorial optimization, and stochastic optimization, and their applications in signal processing for radar and wireless communications.



Daniel P. Palomar (S'99–M'03–SM'08) received the electrical engineering and Ph.D. degrees (both with honors) from the Technical University of Catalonia (UPC), Barcelona, Spain, in 1998 and 2003, respectively.

He is an Associate Professor with the Department of Electronic and Computer Engineering, Hong Kong University of Science and Technology (HKUST), Hong Kong, which he joined in 2006. He had previously held several research appointments, namely, at King's College London (KCL), London, U.K.; UPC; Stanford University, Stanford, CA; Telecommunications Technological Center of Catalonia (CTTC), Barcelona; Royal Institute of Technology (KTH), Stockholm, Sweden; University of Rome "La Sapienza," Rome, Italy; and Princeton University, Princeton, NJ. His current research interests include applications of convex optimization theory, game theory, and variational inequality theory to signal processing and communications.

Dr. Palomar is an Associate Editor of the IEEE TRANSACTIONS ON INFORMATION THEORY, and has been an Associate Editor of the IEEE TRANSACTIONS ON SIGNAL PROCESSING, a Guest Editor of the IEEE SIGNAL PROCESSING MAGAZINE 2010 Special Issue on Convex Optimization for Signal Processing, a Guest Editor of the IEEE JOURNAL ON SELECTED AREAS IN COMMUNICATIONS 2008 Special Issue on Game Theory in Communication Systems, the Lead Guest Editor of the IEEE JOURNAL ON SELECTED AREAS IN COMMUNICATIONS 2007 Special Issue on Optimization of MIMO Transceivers for Realistic Communication Networks. He serves on the IEEE Signal Processing Society Technical Committee on Signal Processing for Communications (SPCOM). He was the General Co-Chair of the 2009 IEEE Workshop on Computational Advances in Multi-Sensor Adaptive Processing (CAMSAP). He is a recipient of a 2004/2006 Fulbright Research Fellowship; the 2004 Young Author Best Paper Award by the IEEE Signal Processing Society; the 2002/2003 Best Ph.D. prize in Information Technologies and Communications by UPC; the 2002/2003 Rosina Ribalba first prize for the Best Doctoral Thesis in Information Technologies and Communications by the Epson Foundation; and the 2004 prize for the Best Doctoral Thesis in Advanced Mobile Communications by the Vodafone Foundation and COIT.

Dr. Palomar is an Associate Editor of the IEEE TRANSACTIONS ON INFORMATION THEORY, and has been an Associate Editor of the IEEE TRANSACTIONS ON SIGNAL PROCESSING, a Guest Editor of the IEEE SIGNAL PROCESSING MAGAZINE 2010 Special Issue on Convex Optimization for Signal Processing, a Guest Editor of the IEEE JOURNAL ON SELECTED AREAS IN COMMUNICATIONS 2008 Special Issue on Game Theory in Communication Systems, the Lead Guest Editor of the IEEE JOURNAL ON SELECTED AREAS IN COMMUNICATIONS 2007 Special Issue on Optimization of MIMO Transceivers for Realistic Communication Networks. He serves on the IEEE Signal Processing Society Technical Committee on Signal Processing for Communications (SPCOM). He was the General Co-Chair of the 2009 IEEE Workshop on Computational Advances in Multi-Sensor Adaptive Processing (CAMSAP). He is a recipient of a 2004/2006 Fulbright Research Fellowship; the 2004 Young Author Best Paper Award by the IEEE Signal Processing Society; the 2002/2003 Best Ph.D. prize in Information Technologies and Communications by UPC; the 2002/2003 Rosina Ribalba first prize for the Best Doctoral Thesis in Information Technologies and Communications by the Epson Foundation; and the 2004 prize for the Best Doctoral Thesis in Advanced Mobile Communications by the Vodafone Foundation and COIT.



Shuzhong Zhang received the B.Sc. degree in applied mathematics from Fudan University in 1984, and the Ph.D. degree in operations research and econometrics from the Tinbergen Institute, Erasmus University, in 1991.

He is a Professor with the Industrial and Systems Engineering Program, University of Minnesota, and is currently on leave from the Department of Systems Engineering and Engineering Management, The Chinese University of Hong Kong. He had held faculty positions with the Department of Econometrics, University of Groningen (1991–1993), and the Econometric Institute, Erasmus University (1993–1999). Since 1999, he has been with Department of Systems Engineering and Engineering Management, The Chinese University of Hong Kong.

Dr. Zhang received the Erasmus University Research Prize in 1999, the CUHK Vice-Chancellor Exemplary Teaching Award in 2001, the SIAM Outstanding Paper Prize in 2003, and the IEEE Signal Processing Society Best Paper Award in 2010. He was an elected Council Member at Large of the Mathematical Programming Society for 2006–2009, and is Vice President of the Operations Research Society of China. He serves on the Editorial Board of five academic journals, including *Operations Research* and the *SIAM Journal on Optimization*.



Alfonso Farina (M'95–SM'98–F'00) received the doctor degree in electronic engineering from the University of Rome (I), Italy, in 1973.

In 1974, he joined Selenia, now SELEX Sistemi Integrati, where he has been a Manager since May 1988. He was Scientific Director in the Chief Technical Office. Currently, he is Director of the Analysis of Integrated Systems Unit. In his professional life, he has provided technical contributions to detection, signal, data, image processing and fusion for the main radar systems conceived, designed, and developed in

the Company. He has provided leadership in many projects—also conducted in the international arena—in surveillance for ground and naval applications, in airborne early warning and in imaging radar. From 1979 to 1985, he has also been a Professor of radar techniques with the University of Naples; in 1985 he was appointed Associate Professor. He is the author of more than 500 peer-reviewed technical publications and the author of books and monographs: *Radar Data Processing* (Vol. 1 and 2) (translated in Russian and Chinese), (U.K.: Researches Studies Press, and New York: Wiley, 1985–1986); *Optimized Radar Processors*, (on behalf of IEE, London, U.K.: Peter Peregrinus, 1987); and *Antenna Based Signal Processing Techniques for Radar Systems*, 1992. He wrote the chapter “ECCM Techniques” in the *Radar Handbook* (2nd ed., 1990, and 3rd ed., 2008), edited by Dr. M. I. Skolnik.

Dr. Farina has been session chairman at many international radar conferences. In addition to lecturing at universities and research centers in Italy and abroad, he

also frequently gives tutorials at the International Radar Conferences on signal, data, and image processing for radar; in particular on multisensor fusion, adaptive signal processing, space-time adaptive processing (STAP), and detection. In 1987, he received the Radar Systems Panel Award of IEEE Aerospace and Electronic Systems Society (AESS) for development of radar data processing techniques. He is the Italian representative of the International Radar Systems Panel of the IEEE AESS. He is the Italian industrial representative (Panel Member at Large) at the Sensor and Electronic Technology (SET) of Research Technology Organisation (RTO) of NATO. He has been on the BoD of the International Society for Information Fusion (ISIF). He has been the Executive Chair of the International Conference on Information Fusion (Fusion) 2006, Florence, Italy, July 10–13, 2006. He has been nominated Fellow of IEEE with the following citation: “For development and application of adaptive signal processing methods for radar systems.” Recently, he has been nominated international fellow of the Royal Academy of Engineering, U.K.; this fellowship was presented to him by HRH Prince Philip, the Duke of Edinburgh. He is a referee of numerous publications submitted to several journals of IEEE, IEE, Elsevier, etc. He has also cooperated with the Editorial Board of the IEE *Electronics & Communication Engineering Journal*. More recently, he has served as a member of the Editorial Board of *Signal Processing* (Elsevier) and has been Co-Guest Editor of its Special Issue on New Trends and Findings in Antenna Array Processing for Radar, September 2004. He is the corecipient of the following Best Paper Awards: entitled to B. Carlton of the IEEE TRANSACTIONS ON AEROSPACE AND ELECTRONIC SYSTEMS for 2001 and 2003 and also of the International Conference on Fusion 2005. He has been the leader of the team that received the 2002 AMS CEO award for Innovation Technology. He has been the corecipient of the AMS Radar Division award for Innovation Technology in 2003. Moreover, he has been the corecipient of the 2004 AMS CEO Award for Innovation Technology. He has been the leader of the team that won the 2004 First Prize Award for Innovation Technology of Finmeccanica, Italy. This award context has seen the submission of more than 320 projects. This award has been set for the first time in 2004. In September 7, 2006, he received the Annual European Group Technical Achievement Award 2006 by the European Association for Signal, Speech and Image Processing (EURASIP), with the citation: “For development and application of adaptive signal processing technique in practical radar systems.” In 2006 and 2009, he was a corecipient of the annual Innovation Technology award of SELEX Sistemi Integrati. He has been appointed member in the Editorial Boards of *IET Radar, Sonar and Navigation and of Signal, Image, and Video Processing Journal* (SIVP). He has been the General Chairman of the IEEE Radar Conference 2008, Rome, May 26–30, 2008. He is a Fellow of the Institution of Engineering and Technology (IET), UK. He has been recently nominated Fellow of EURASIP, the citation reads: “For contributions to radar system design, signal, data and image processing, data fusion and particularly for the development of innovative algorithms for deployment into practical radar systems.” He is also the recipient of the 2010 IEEE Dennis J. Picard Gold Medal for Radar Technologies and Applications with the following citation: “For continuous, innovative, theoretical and practical contributions to radar systems and adaptive signal processing techniques.”